

1 TITLE – Revised Manuscript, submitted 1 April 2010

2 Isotopic Anomalies in Organic Nanoglobules from Comet 81P/Wild 2: Comparison to Murchison
3 Nanoglobules and Isotopic Anomalies Induced in Terrestrial Organics by Electron Irradiation

4

5 AUTHORS

6 Bradley T. De Gregorio*^{a,b}

7 Rhonda M. Stroud^b

8 Larry R. Nittler^c

9 Conel M. O’D. Alexander^c

10 A. L. David Kilcoyne^d

11 Thomas J. Zega^b

12 ^aNaval Research Laboratory/National Research Council Cooperative Research Fellow

13 ^bMaterials Science and Technology Division, Code 6366, U.S. Naval Research Laboratory, 4555 Overlook
14 Ave. SW, Washington, DC 20375-5320 (E-mail: bradley.degregorio.ctr@nrl.navy.mil;

15 rhonda.stroud@nrl.navy.mil; thomas.zega@nrl.navy.mil)

16 ^cDepartment of Terrestrial Magnetism, Carnegie Institution of Washington, 5241 Broad Branch Rd. NW,
17 Washington, DC 20015 (E-mail: lnittler@ciw.edu; alexander@dtm.ciw.edu)

18 ^dAdvanced Light Source, Lawrence Berkeley National Laboratory, Mail Stop 7R0222, 1 Cyclotron Rd.,
19 Berkeley, CA 94720-8225 (E-mail: alkilcoyne@lbl.gov)

20 *Corresponding author - Phone: (202) 767-2079; Fax: (202) 767-1697; E-mail:

21 bradley.degregorio.ctr@nrl.navy.mil

22

23

24 ABSTRACT

25 Nanoglobules are a form of organic matter found in interplanetary dust particles and primitive
26 meteorites and are commonly associated with ^{15}N and D isotopic anomalies that are suggestive of
27 interstellar processes. We report the discovery of two isotopically anomalous organic globules from the
28 Stardust collection of particles from Comet 81P/Wild 2 and compare them with nanoglobules from the
29 Murchison CM2 meteorite. One globule from Stardust Cometary Track 80 contains highly aromatic
30 organic matter and a large ^{15}N anomaly ($\delta^{15}\text{N} = 1120\%$). Associated, non-globular, organic matter from
31 this track is less enriched in ^{15}N and contains a mixture of aromatic and oxidized carbon similar to bulk
32 insoluble organic material (IOM) from primitive meteorites. The second globule, from Cometary Track 2,
33 contains non-aromatic organic matter with abundant nitrile ($-\text{C}\equiv\text{N}$) and carboxyl ($-\text{COOH}$) functional
34 groups. It is significantly enriched in D ($\delta\text{D} = 1000\%$) but has a terrestrial $^{15}\text{N}/^{14}\text{N}$ ratio. Experiments
35 indicate that similar D enrichments, unaccompanied by ^{15}N fractionation, can be reproduced in the
36 laboratory by electron irradiation of epoxy or cyanoacrylate. Thus, a terrestrial origin for this globule
37 cannot be ruled out, and, conversely, exposure to high-energy electron irradiation in space may be an
38 important factor in producing D anomalies in organic materials. For comparison, we report two
39 Murchison globules: one with a large ^{15}N enrichment and highly aromatic chemistry analogous to the
40 Track 80 globule and the other only moderately enriched in ^{15}N with IOM-like chemistry. The
41 observation of organic globules in Comet 81P/Wild 2 indicates that comets likely sampled the same
42 reservoirs of organic matter as did the chondrite parent bodies. The observed isotopic anomalies in the
43 globules are most likely preserved signatures of low temperature ($<10\text{ K}$) chemistry in the interstellar
44 medium or perhaps the outer regions of the solar nebula. In other extraterrestrial samples, D isotopic
45 anomalies, but not those of ^{15}N , may be explained in part by exposure to ionizing electron radiation.

46

47 KEYWORDS

48 Stardust, nanoglobule, organic matter, comet, isotopic anomaly, primitive meteorite

49

50

51 TEXT

52 **1. INTRODUCTION**

53 In 2006, NASA's Stardust spacecraft returned over 10^4 micrometer-sized particles from the dust
54 tail of comet Wild 2 (Brownlee et al., 2006). Prior to their return, the cometary samples were anticipated
55 to contain abundant presolar materials, including interstellar material and grains that formed around
56 other stars or supernovae. Preliminary examination of Wild 2 returned samples indicated that the comet
57 contains a non-equilibrium assemblage of material, including refractory crystalline materials that likely
58 formed in the inner regions of the early solar nebula and only minor amounts of presolar grains
59 (Brownlee et al., 2006; McKeegan et al., 2006). Although the majority of the currently analyzed
60 cometary dust is comprised of silicate and sulfide minerals (Zolensky et al., 2006), a portion contains
61 organic and other carbonaceous matter (Sandford et al., 2006) in the form of carbonaceous grains (Cody
62 et al., 2008a), carbonaceous rims surrounding other minerals (Matrajt et al., 2008), and volatile organics
63 diffused into the silica aerogel capture medium (Glavin et al., 2008). Organic matter that exhibits large
64 excesses in D or ^{15}N isotopes relative to H and ^{14}N , respectively, compared to terrestrial isotopic ratios, is
65 present in many extraterrestrial materials, such as carbonaceous chondrite meteorites (Busemann et al.,
66 2006) and interplanetary dust particles (IDPs; Messenger, 2000; Floss et al., 2004; Keller et al., 2004).
67 These anomalous isotopic enrichments are interpreted to be likely signatures of primordial chemistry
68 that occurred in the proto-solar molecular cloud or in the outer cold regions of the solar system. The
69 most extreme isotopic enrichments are commonly concentrated within μm to sub- μm "hotspots",
70 suggesting the presence of a granular organic carrier of the isotopic anomalies. Similar isotopic
71 enrichments have only been observed in a few of the Stardust samples (Sandford et al., 2006; Matrajt et
72 al., 2008; Stadermann et al., 2008).

73 Spherical, and typically hollow, sub- μm carbonaceous grains occur in various carbonaceous
74 chondrite meteorites (Garvie and Buseck, 2004, 2006; Nakamura-Messenger et al., 2006) and have

75 recently been reported in chondritic porous IDPs (Messenger et al., 2008; Busemann et al., 2009). These
76 “nanoglobules” range in diameter from less than 50 nm up to 2 μm (Nakamura-Messenger et al., 2006).
77 Nanoglobules in the Tagish Lake and Bells meteorites were shown to contain large ^{15}N and D
78 enrichments and compose a portion of the isotopic hotspots observed in these meteorites (Ashley et al.,
79 2005; Nakamura-Messenger et al., 2006; Messenger et al., 2008). Extraterrestrial organic matter may
80 acquire ^{15}N and D isotopic enrichments in cold interstellar or outer solar nebular environments through
81 gas-phase reactions (Aikawa and Herbst, 1999; Sandford et al., 2001; Rodgers and Charnley, 2008a, b)
82 and ion-surface reactions on icy grains (Tielens, 1983). Several mechanisms have been hypothesized to
83 explain the formation of a hollow globular morphology from isotopically-enriched organic matter.
84 Organic nanoglobules may form via UV irradiation of organic-rich interstellar ice grains, followed by
85 sublimation of the interior ice (Nakamura-Messenger et al., 2006). Alternatively, organic molecules that
86 are amphipathic, i.e. possessing both hydrophilic and hydrophobic properties, may spontaneously form
87 hollow spherical structures. Upon exposure to aqueous fluids, the hydrophobic portions of such
88 molecules aggregate in order to exclude all interaction with water, while the hydrophilic portions spread
89 out to form a protective barrier around the hydrophobic core. Amphipathic organic matter may be
90 synthesized by UV photolysis or other radiation processing of common interstellar organic molecules in
91 ice grains, and they have been shown to self-organize into globules when dispersed in water (Dworkin et
92 al., 2001). Spherical globules may also be created during aqueous alteration on meteorite parent bodies
93 (Cody et al., 2009), but this process would be less likely to occur on cometary bodies unless, contrary to
94 expectations, they also experienced significant episodes in which liquid water was present.

95 The ubiquity of nanoglobules in other primitive extraterrestrial samples suggests that they
96 should also be present in comets. In the Wild 2 samples, however, only one spherical carbonaceous
97 feature has been reported to date (Matrajt et al., 2008), and although it contains an isotopic anomaly, it
98 encompasses a sulfide grain as a “rind”, unlike all observed globules in meteorites and IDPs, which do

99 not envelop mineral grains. Here we report two organic globular features found in Comet 81P/Wild 2
100 samples that exhibit distinct chemical and isotopic signatures, and we compare them with nanoglobules
101 from the Murchison meteorite. The ^{15}N or D isotopic anomalies present in these objects may indicate a
102 very primitive, and possibly presolar, heritage. However, we cannot unambiguously rule out the
103 possibility that one of the Stardust globules is terrestrial contamination because we have also found that
104 similar D enrichments can be induced by transmission electron microscopy (TEM) of some organic
105 materials.

106

107

2. MATERIALS AND METHODS

108

2.1. Sample preparation

109

110

111

112

113

114

115

116

117

118

119

120

121

Several particles extracted from the bulb-like region of Cometary Track 80 were allocated from the Stardust collection at NASA Johnson Space Center (JSC). Particle C2092,6,80,43,0 (Track 80, Particle 43) was transferred via a fresh glass needle into a molten sulfur droplet, which then crystallized around the particle upon cooling. The sulfur droplet was attached to the tip of an epoxy stub with a cyanoacrylate adhesive and sectioned with a diamond knife in an ultramicrotome at the Carnegie Institution of Washington (CIW). Several 90 nm thick slices were transferred to a 200 mesh thin-bar Cu TEM grid with a SiO support film. Since this was the second TEM grid containing ultramicrotome sections of the particle, it was designated C2092,6,80,43,2. The sulfur was removed by sublimation in a 60 °C oven overnight. At no point in this process was the sample exposed to a high-energy particle beam or temperatures greater than 140° C, which is the maximum temperature used to melt the sulfur droplet.

A second sample, FC3,0,2,4,5 (Track 2, Particle 4), was prepared in a similar manner by Keiko Nakamura-Messenger at JSC prior to allocation as part of the preliminary examination of the Stardust samples.

122 For comparison with the Wild 2 samples, we also studied fresh ultramicrotomed sections of
123 insoluble organic matter (IOM) from the Murchison (CM2) meteorite, created from a sulfur-embedded
124 residue. This material has already been well-characterized by a variety of methods (Alexander et al.,
125 1998, 2007; Cody and Alexander, 2005; Cody et al., 2008b) and is known to contain D and ¹⁵N isotopic
126 hotspots (Busemann et al., 2006), which may be associated with nanoglobules observed in other
127 residues from this meteorite (Garvie and Buseck, 2004; Garvie, 2006). The ultramicrotomed sections of
128 Murchison IOM were placed on the same type of SiO-coated TEM grids as the cometary samples, and
129 the sulfur was removed by sublimation in a 70 °C oven for several hours.

130

131 **2.2. X-ray absorption near-edge structure spectroscopy (XANES)**

132 Samples were analyzed by synchrotron-based scanning-transmission X-ray microscopy (STXM) at
133 beamline X1A1 at the National Synchrotron Light Source (NSLS), Brookhaven National Laboratory (BNL),
134 and beamline 5.3.2 at the Advanced Light Source (ALS), Lawrence Berkeley National Laboratory (LBNL).
135 Both instruments allow XANES analysis at the C 1s absorption edge, but the STXM instrument at ALS can
136 additionally be tuned for N 1s or O 1s analyses (Kilcoyne et al., 2003). Organic matter in microtomed
137 samples was distinguished from the aerogel capture medium and other inorganic material by acquiring
138 X-ray absorption images at energies above and below the C 1s absorption edge (e.g. 290 eV and 280 eV).
139 Since most carbonaceous matter will begin to absorb X-rays at energies above 284 eV, organic matter
140 could be observed in the 290 eV images but was absent in the 280 eV images.

141 C-XANES spectra were acquired by first recording a series of X-ray absorption images at photon
142 energies between 270 eV and 320 eV with an energy step between subsequent images as small as 0.1
143 eV (Jacobsen et al., 2000). Prior to STXM analyses, the microscope was calibrated to well-known carbon
144 and oxygen photoabsorptions of CO₂, and this initial calibration was not observed to drift more than 0.1
145 eV over the course of the analyses. The pixel size in the X-ray images was set to 25 nm, near the

146 maximum instrumental resolution of the microscope. Each column of pixels in an aligned image “stack”
147 then represents a full X-ray absorption spectrum for that coordinate. Principal component analysis,
148 followed by component cluster analysis, was used to select regions of interest with similar spectra
149 within the image stack (Lerotic et al., 2004). From these data, an average XANES optical density (*OD*)
150 was calculated by $OD(E) = -\log[I(E)/I_0(E)]$, where $I(E)$ and $I_0(E)$ are the average transmitted X-ray intensity
151 of the sample and background, respectively, at a given energy E . This method also allows for subtraction
152 of contributions from amorphous carbon coatings deposited on the sample to mitigate charging effects
153 from high-energy electrons during transmission electron microscopy (TEM). At ALS, the procedures for
154 acquiring N- and O-XANES spectra are similar to those for C-XANES but at higher photon energies (N
155 absorbs above 397 eV and O absorbs above 529 eV).

156

157 **2.3. Transmission electron microscopy (TEM)**

158 Samples were analyzed with a JEOL 2200FS field-emission TEM at the Naval Research Laboratory
159 (NRL) at an operating voltage of 200 keV. For this particular study, bright-field TEM imaging was used to
160 observe the morphology of the globules at much higher spatial resolution than that achievable by STXM.
161 An energy dispersive X-ray spectrometer (EDS) attached to the TEM allowed the distinction between
162 organic matter and spacecraft aerogel by sample morphology and composition (Stroud et al., 2004).
163 Although a carbon-free SiO support film was beneficial for C-XANES analysis, such a non-conducting film
164 charges under the electron beam. To mitigate sample charging in the TEM, a thin amorphous carbon
165 coat was deposited on the back side of the TEM grid.

166 Murchison IOM samples were analyzed by TEM prior to XANES analysis in order to identify and
167 locate appropriate nanoglobule targets. TEM analyses were performed primarily at low magnifications
168 and with small condenser apertures to minimize the total electron fluence to which the sample was
169 exposed (approximately 10^3 electrons/nm² at a fluence rate of about 2 mA/cm²). Comparison of XANES

170 spectra for bulk Murchison IOM acquired both before and after TEM analysis indicates that this minimal
171 TEM electron fluence does not significantly alter the bulk chemistry.

172 We also performed a set of experiments to address concerns that exposure to electron
173 irradiation during TEM analysis could artificially induce D or ¹⁵N isotopic enrichments in organic samples.
174 We prepared ultramicrotome sections of cyanoacrylate adhesive and epoxy and exposed them to the
175 electron beam under controlled conditions. These samples were chosen because cyanoacrylate shares
176 XANES spectral features with the Track 2 sample (FC3,0,2,4,5), as described below. Cyanoacrylate and
177 epoxy are possible laboratory contaminants during sample preparation and can exhibit contrast changes
178 during exposure to the high-energy electron beam, most likely as removal of hydrogen.

179 Ultramicrotomed cyanoacrylate and epoxy sections were placed on Quantifoil Cu TEM grids containing a
180 perforated amorphous carbon support film. Several small regions within these sections were exposed to
181 the 200 keV electron beam to mimic typical analyses of Stardust samples, which may include high-
182 resolution imaging, EDS or electron energy-loss spectroscopy (EELS) analysis using a converged beam,
183 and hyperspectral EDS mapping in scanning (STEM) mode, each of which may contribute large electron
184 fluences. In conventional TEM mode, a 1.5 μm circular region was irradiated for ~30 minutes with a
185 semi-converged beam at 10,000X magnification, resulting in a total electron fluence of approximately
186 10⁸ electrons/nm² at a fluence rate of about 500 mA/cm². In STEM mode, a converged beam with a
187 nominal 1 nm probe size and 0.9 nA probe current was rastered over a 15 μm by 15 μm square region
188 for ~60 minutes, resulting in an electron fluence of approximately 10⁵ electrons/nm² at a fluence rate of
189 about 10⁵ A/cm². These STEM beam conditions are typical for the acquisition of an EDS hyperspectral
190 map for a 10 μm Wild 2 particle. These samples were compared with adjacent ultramicrotome sections
191 not exposed to the TEM beam in order to measure any differences in isotopic composition between the
192 two samples.

193

194 **2.4. Secondary ion mass spectrometry (SIMS)**

195 Hydrogen, carbon, and nitrogen isotopic compositions of the samples were measured with a
196 Cameca NanoSIMS 50L ion microprobe in the Department of Terrestrial Magnetism at the CIW. TEM
197 grids were first attached to Al stubs with colloidal Ag paint and then coated with a thin layer of Au to
198 eliminate charging effects. A focused 16 keV Cs⁺ primary ion beam was rastered over the samples and
199 negative secondary ion images were acquired simultaneously in multi-collection mode. Measurements
200 were made in two steps. In the first, a ~1 pA, 150 nm beam was used to acquire images of ¹²C, ¹³C,
201 ¹²C¹⁴N, ¹²C¹⁵N, ²⁸Si, and secondary electrons. In the second step, a slightly higher beam current (~3 pA,
202 300 nm beam) was used to acquire images of H, ²H, ¹²C, and secondary electrons. The mass resolution of
203 the instrument was sufficient to resolve all significant isobaric interferences. Well-characterized
204 insoluble organic matter (IOM) from the carbonaceous chondrite GRO 95577 (Alexander et al., 2007)
205 was used to calibrate the instrumental fractionation for carbon and nitrogen isotopic ratios and the
206 relative sensitivity factor used to convert CN⁻/C⁻ ratios to N/C atomic ratios. A terrestrial organic
207 standard was used to calibrate D/H measurements. Isotopic compositions and average atomic N/C ratios
208 of sub-regions in the ion images were quantitatively calculated with the L'Image software package (L.
209 Nittler, CIW). Reported errors are based purely on counting statistics. The globule samples were, for all
210 practical purposes, consumed during the NanoSIMS analyses.

211

212

3. RESULTS

213 **3.1. Sample morphology**

214 One of the microtomed sections of sample C2092,6,80,43,2 (Track 80) consists of organic matter
215 surrounded by compressed aerogel on two sides (Figure 1A, hereafter identified as Track 80 organic
216 section) and an adjacent carbonaceous globular feature (Figure 1B, hereafter identified as Track 80
217 globule). The intimate association of organic matter and aerogel in the Track 80 organic section suggests

218 that it is cometary material captured by the Stardust spacecraft. Spot EDS analyses confirm that the
219 center of the Track 80 organic section is composed primarily of carbonaceous matter, while the
220 surrounding aerogel in the Track 80 organic section contains higher silica abundance. Carbonaceous
221 matter is also present within the surrounding aerogel above background levels, indicating the presence
222 of cometary organic matter infiltrating the aerogel.

223 The Track 80 globule is roughly circular with an outer diameter of 1.4 μm and a wall thickness of
224 approximately 450 nm. The center is not fully hollow but is consistent with a 90 nm thick
225 ultramicrotome section sampling one end of a hollow, spherical object. The globule walls are
226 homogeneous with no apparent layering or evidence of graphitization in higher-resolution images. The
227 close proximity of the Track 80 globule to the nearby organic section (2.5 μm) suggests that the two
228 features must have been present in the same ultramicrotome slice rather than in separate slices. Most
229 likely, the globule was initially attached to the organic section and was later separated during
230 ultramicrotomy. Various sectioning effects may result in small relative movements of material in sulfur-
231 embedded ultramicrotome sections, including brittle failure of the surrounding crystalline sulfur,
232 changes in hardness or density of the embedded sample, and periodic compression of sample and/or
233 sulfur (Malis and Steele (1990)).

234 Sample FC3,0,2,4,5 (Track 2) contains a few scattered microtomed slices of aerogel with no
235 apparent cometary material. However, a globular feature is located near some of the aerogel slices
236 (Figure 1C, hereafter identified as Track 2 globule). The sample is wedge-shaped, decreasing in thickness
237 to the lower left, with smooth, flat surfaces, indicating that it has been ultramicrotomed. The globule is
238 2.3 μm in diameter with a wall thickness of approximately 700 nm. Unlike the Track 80 globule, the
239 Track 2 globule is completely hollow in the center, but TEM images show increasing sample thickness
240 from the center out to a 450 nm radius where image contrast becomes roughly constant, indicating the

241 true void area of the globule. Again, this globule is homogenous and does not show any layering or
242 graphitization.

243 Several organic nanoglobules were identified in the Murchison IOM sample and analyzed by
244 TEM, STXM, and SIMS. Two adjacent globules of particular interest are shown in Figure 1D. Both
245 globules are partially hollow with approximately 100 nm thick walls. The larger (lower) globule
246 (hereafter identified as M1) has an outer diameter of 500 nm, while the smaller globule (hereafter
247 identified as M2) has an outer diameter of 350 nm. A detailed discussion of the entire Murchison
248 dataset and data for other meteoritic IOM residues will be presented elsewhere.

249

250 **3.2. Organic chemistry**

251 All of the microtomed Track 80 material, including the associated aerogel, strongly absorbs X-
252 rays at 290 eV, indicating the presence of abundant carbonaceous material. Both the cometary organic
253 matter and that associated with aerogel in the Track 80 organic section exhibit identical XANES spectra
254 (Figure 2A), each containing three peaks due to $1s \rightarrow \pi^*$ (anti-bonding) electronic transitions involving
255 doubly-bonded C atoms at 285.0 eV, 286.7 eV, and 288.5 eV, followed by a $1s \rightarrow \sigma^*$ (anti-bonding)
256 absorption edge. The 285.0 eV π^* absorption is characteristic of aromatic carbon-carbon bonding (C=C)
257 and polyaromatic domains, while carboxylic acid functional groups (-COOH) generate a well-established
258 absorption peak at 288.5 eV (Urquhart and Ade, 2002). Photoabsorption at 286.7 eV could be due to
259 several functional groups, including enol or phenol groups ($C_{\text{aromatic}}\text{-OH}$; Cody, 2000; Boyce et al., 2002),
260 vinyl ketone groups ($C_{\text{aromatic}}\text{-C=O}$; Cody et al., 2008a, 2008b; Hitchcock et al., 1992), aromatic amine or
261 amide groups ($C_{\text{aromatic}}\text{-N}$; Ade and Urquhart, 2002), or nitrile groups ($\text{-C}\equiv\text{N}$; Hitchcock et al., 2001; Ade
262 and Urquhart, 2002). Since carboxyl functionality is already present in this material, it is likely that the
263 286.7 eV absorption feature is due to additional carbon-oxygen bonding, although it is possible that
264 specific carbon-nitrogen bonding may significantly contribute to this feature. Enols and phenols can also

265 transform into ketones and other carbonyls under X-ray and electron beams (Cody, 2000). The C-XANES
266 spectrum of the Track 80 organic section appears similar to typical meteoritic insoluble organic matter
267 (Cody et al., 2008b), represented by the Murchison spectrum in Figure 2.

268 In contrast, the Track 80 globule (Figure 2B) exhibits a distinct C-XANES spectrum from the
269 nearby Track 80 organic section. The C-XANES spectrum for this globule shows evidence of saturation
270 (flattening) due to the almost complete absorption of X-rays relative to background intensity ($I/I_0 \approx 0$),
271 most likely because the section thickness exceeds the average penetration depth of low energy X-rays.
272 Despite this, a broad aromatic peak is still visible at 285.4 eV. The shape of this peak suggests
273 contributions from at least two organic moieties: polyaromatic domains contributing around 285.0 eV
274 and modified aromatic molecules with photoabsorptions shifted to slightly higher X-ray energies. A
275 smaller peak at 291.0 eV could be related to the characteristic $1s \rightarrow \sigma^*$ (anti-bonding) electronic
276 transition at 291.6 eV from large polyaromatic domains or graphene sheets that is sometimes referred
277 to as a graphite exciton (Weng et al., 1989; Brühwiler et al., 1995; Ahuja et al., 1996; Wessely et al.,
278 2005). The strength of the graphite exciton peak has been correlated to the extent of thermal
279 metamorphism on meteorite parent bodies (Cody et al., 2008b), but it may be suppressed depending on
280 the orientation or disorder of the graphitic domains (Rosenberg et al., 1986; Skytt et al., 1994; Gago et
281 al., 2001; Belavin et al., 2006). The broad aromatic peak observed in the globule spectrum is not
282 consistent with the sharp aromatic peak observed in thermally-processed graphitized material, and
283 therefore, the 291.0 eV peak is most likely due to the partial alignment of polyaromatic domains. The
284 spectra may contain contributions from carboxyl functional groups at 288.5 eV, but potential
285 contributions from enols and aromatic ketones are masked by the large aromatic π^* photoabsorption.
286 Unlike the Track 80 organic section, the Track 80 globule appears to be dominated by aromatic carbon.
287 However, because no crystal lattice fringes, and in particular no 3.4 Å lattice fringes characteristic of the

288 (0002) d-spacing for graphite, were observed by TEM, the aromatic carbon most likely comprises
289 randomly oriented polyaromatic moieties similar to polycyclic aromatic hydrocarbons (PAHs).

290 The Track 2 globule appears to consist of a third type of N-rich organic matter. The initial C-
291 XANES spectrum of this globule contains photoabsorptions at 286.7 eV and at 288.6 eV, but no aromatic
292 285.0 eV absorption (Figure 3A). After exposure to the 200 keV electron beam during TEM analysis, the
293 organics show evidence of damage—a 285 eV “shoulder” is present and the major peaks have
294 decreased in intensity, most notably the 288.6 eV peak (Figure 3B). The increased photoabsorption
295 around 285 eV and 291 eV suggests that the primary damage mechanism is the cyclization of aliphatic
296 carbon to form polyaromatic domains, with a concurrent loss of hydrogen atoms. As before, the 288.6
297 eV peak most likely arises from abundant carboxyl functional groups. However, the sharp 286.7 eV peak
298 contains a large contribution from nitrile functional groups in addition to enols and ketones. This is
299 corroborated by the dominant $1s \rightarrow \pi^*$ photoabsorption at 399.8 eV in the N-XANES spectrum (Figure
300 3C; Shard et al., 2004; Leinweber et al., 2007; Cody et al., 2008a). Imine (C=N) bonds in aromatic
301 imidazoles and purines may also generate a N-XANES peak at 399.8 eV (Apen et al., 1993; Leinweber et
302 al., 2007), but since an imine photoabsorption is not observed around 286.0 eV in C-XANES, aromatic
303 heterocycles with more than one N atom are not common in the Track 2 globule. However, the π^* peak
304 at 398.6 eV can be reliably attributed to aliphatic imine bonds and aromatic heterocycles containing a
305 single N atom (Jokic et al., 2004; Leinweber et al., 2007; Cody et al., 2008a). The third N-XANES peak at
306 401.2 eV can either be due to pyrrolic N in imidazoles and purines (Apen et al., 1993; Leinweber et al.,
307 2007) or amide ($O=C-NH_x$) functional groups (Gordon et al., 2003; Cooper et al., 2004; Jokic et al., 2004;
308 Leinweber et al., 2007). Because the lack of a major C-XANES photoabsorption around 286.0 eV
309 indicates that aromatic heterocycles with more than one N atom are not present in high abundance, we
310 attribute the N-XANES peak at 401.2 eV to amide functionality and possible peptide-like bonding. We
311 note that the N-XANES spectrum was acquired after the organic matter was damaged during TEM

312 imaging, and therefore the relative abundances of N-containing functional groups inferred from the N-
313 XANES spectrum very likely do not represent the abundances present in the original undamaged
314 globule. In particular, beam damage of amino acids has been shown to create aromatic carbon, imine,
315 and nitrile bonding (Zubavichus et al., 2004). However, the pre-damage C-XANES spectrum (Figure 3A)
316 clearly shows the presence of nitrile functional groups. Using the method described by Cody et al.
317 (2008a), an atomic N/C ratio of 0.13 is calculated for this globule based on the XANES data.

318 The undamaged C-XANES spectrum of the Track 2 globule is nearly identical to that of common
319 cyanoacrylate adhesive (Figure 3), in which the photoabsorptions at 286.7 eV and 288.6 eV correspond
320 to the presence of nitrile and carboxyl functional groups, respectively. A cyanoacrylate adhesive was
321 used during sample preparation of both Stardust samples, and ultramicrotomed sections of
322 cyanoacrylate are often present on sulfur-embedded Stardust sample mounts in the proximity of
323 authentic cometary material if the cyanoacrylate formed a thin layer over the sides or top of the
324 crystallized sulfur droplet. Cyanoacrylate strips may also be purposely laid on TEM grids to mark the
325 position of sulfur-embedded, microtomed Stardust particles, which may be difficult to locate otherwise
326 once the surrounding sulfur has been removed. While we have often seen triangular, trapezoidal, or
327 semicircular cyanoacrylate sections, we have not previously observed circular or globular sections in our
328 ultramicrotomed samples, but they may, in principle, result from sectioning of small droplets or bubbles.

329 The two Murchison nanoglobules (M1 and M2) also contain distinct organic chemistries. The
330 smaller of the two globules (M2), as well as the majority of the other Murchison globules characterized
331 by STXM (not described in this study), show C-XANES spectra similar to that of the bulk Murchison IOM,
332 with photoabsorptions at 285 eV, 286.7 eV, and 288.6 eV, corresponding to aromatic bonding, aromatic
333 ketone and enol bonding, and carboxyl functional groups, respectively (Figure 2D). However, the C-
334 XANES spectrum of the larger Murchison globule (M1) is similar to that of the Stardust Track 80 globule,
335 dominated by an aromatic peak at 285.4 eV (Figure 2C). This aromatic Murchison globule spectrum does

336 not appear to be saturated like that of the aromatic Track 80 globule. Furthermore, the Murchison
337 globule (M1) spectrum does not include a distinct exciton peak as seen in the Track 80 globule, but
338 rather contains a well-developed σ^* peak above the C 1s absorption edge that is typical of graphite and
339 highly aromatic material (Cody et al., 2008b). However, since graphitic lattice fringes were not observed
340 during TEM, the M1 globule is likely composed of non-graphitic, aromatic organic matter.

341

342 **3.3. Isotopic composition**

343 Isotopic compositions of hydrogen, carbon, and/or nitrogen were measured in each of the
344 organic globules and in the Track 80 organic section (Table 1). Not all elements were measured in each
345 sample. The Track 80 globule is highly enriched in ^{15}N , with an average $\delta^{15}\text{N}$ value of $+1120 \pm 30\text{‰}$
346 (Figure 1B) that is within the range observed spectroscopically for CN in cometary comae ($+930 \pm 400\text{‰}$;
347 Schulz et al., 2008). It is also moderately depleted in ^{13}C ($\delta^{13}\text{C} = -77 \pm 13\text{‰}$). The Track 80 organic section
348 is also significantly enriched in ^{15}N ($\delta^{15}\text{N} \approx +140\text{‰}$), albeit to a lesser degree than observed in the
349 globule. The nitrogen isotopic composition in this section is heterogeneous on a sub- μm scale, and the
350 largest ^{15}N enrichments occur in aerogel-free areas (Figure 1A). Individual ~ 400 nm hotspots contain
351 above-average $\delta^{15}\text{N}$ values up to $+360 \pm 70\text{‰}$. Based on CN^-/C^- ratios measured with the NanoSIMS, the
352 Track 80 samples have atomic N/C ratios of 0.10-0.15. These values are significantly higher than typical
353 IOM from primitive meteorites (<0.05 ; Alexander et al., 2007), but they are similar to a few N-rich
354 nanoglobules from primitive meteorites (Garvie and Buseck, 2004) and several carbonaceous Wild 2
355 samples (Sandford et al., 2006; Cody et al., 2008a). Unfortunately, failure of the support film during
356 NanoSIMS analysis precluded a robust measurement of D/H ratios within the Track 80 samples, but the
357 partial dataset shows no evidence for a D enrichment greater than about 1000‰ in the Track 80
358 globule. However, this is not a stringent upper limit, since the highly aromatic nature of this globule
359 suggests a relatively low intrinsic H/C ratio, potentially making the sample more susceptible to terrestrial

360 contamination in the NanoSIMS. Nonetheless, it is highly unlikely that the Track 80 globule had a D
361 enrichment comparable to the extreme values observed in isotopic hotspots in meteoritic and IDP
362 organic matter.

363 In contrast to the Track 80 globule, the Track 2 globule contains a nitrogen isotopic composition
364 ($\delta^{15}\text{N} = -7 \pm 5\text{‰}$) that is indistinguishable from terrestrial values and a carbon isotopic composition ($\delta^{13}\text{C}$
365 $= -35 \pm 3\text{‰}$) that is within the typical range of meteoritic IOM (Alexander et al., 1998, 2007). However,
366 this globule does contain a clearly anomalous D/H ratio, with an average $\delta\text{D} = +1000 \pm 170\text{‰}$ (Figure 1C).
367 Apparent variations in D/H in this sample shown in Figure 1C are not statistically significant. The Track 2
368 globule is also N-rich, with an atomic N/C ratio between 0.08 and 0.16, based on NanoSIMS analysis, in
369 good agreement with the value of 0.13 derived from XANES. This N/C ratio is comparable to that found
370 in the Track 80 globule as well as in other carbonaceous Wild 2 samples (Sandford et al., 2006; Cody et
371 al., 2008a). However, this value is slightly lower than the N/C ratio for cyanoacrylate (0.17-0.20). Since
372 these measurements were performed following TEM-induced beam damage evident by XANES, it is
373 possible that TEM analysis could have driven significant nitrogen loss within the sample. If this is the
374 case, then the original N/C ratio of the Track 2 globule could have been higher.

375 Many of the Murchison nanoglobules analyzed with the NanoSIMS in this study have enhanced
376 $^{15}\text{N}/^{14}\text{N}$ ratios (only two of which are described here), relative to the bulk IOM value of $\delta^{15}\text{N} = -1\text{‰}$
377 (Alexander et al., 2007). In particular, the larger of the two globules (M1) in Figure 1D, comprised
378 predominantly of aromatic organic matter as determined by XANES (Figure 2C), exhibits the largest ^{15}N
379 enrichment, with an average $\delta^{15}\text{N} = +470 \pm 35\text{‰}$. The smaller globule (M2), comprised of more oxidized
380 and aliphatic organic matter (Figure 2D), contains a smaller, but still anomalous, ^{15}N enrichment ($\delta^{15}\text{N} =$
381 $+289 \pm 39\text{‰}$). Unfortunately, this TEM grid received a carbon coat directly onto the sample rather than
382 onto the backside of the SiO support film prior to TEM observations. The infiltration of the carbon
383 coating into the porous IOM precluded the accurate measurement of carbon isotopic compositions and

384 atomic N/C ratios for the Murchison globules. In addition, failure of the support film precluded adequate
385 D/H measurements.

386 To test whether the D enrichment measured in the Track 2 globule could be an artifact of
387 extensive TEM beam damage and hydrogen loss in cyanoacrylate, the D/H and $^{15}\text{N}/^{14}\text{N}$ isotopic
388 compositions were analyzed in both electron-irradiated and pristine ultramicrotomed sections of
389 cyanoacrylate adhesive and epoxy. A 15 μm by 15 μm region of cyanoacrylate exposed in scanning
390 (STEM) mode was found to be enriched in D by 500-800‰ relative to non-irradiated material (Figure 4A,
391 B). Similarly, a 3 μm damage spot in epoxy caused by a defocused TEM beam at 10,000X magnification
392 was fractionated with a $\delta\text{D} \approx 1000\text{‰}$ relative to non-irradiated epoxy (Figure 4C, D). In contrast, no
393 significant nitrogen isotopic fractionation ($> 1\text{‰}$) of these samples was observed.

394

395

4. DISCUSSION

4.1. Cometary and meteoritic organic globules

397 The features described here are the first organic nanoglobules, similar to those observed in
398 carbonaceous chondrites and IDPs, reported in the Stardust return samples from comet Wild 2. Matrajt
399 et al. (2008) reported a donut-shaped carbonaceous feature enriched in ^{15}N in the terminal particle from
400 Stardust Track 57 (particle "Febo"). However, this material was observed as a carbonaceous rind
401 surrounding a sulfide grain, and no meteoritic nanoglobules have been observed to contain such
402 embedded mineral grains. The two Stardust globules described in this study are physically, chemically,
403 and isotopically distinct from nearby cometary organic matter. Although both globules have much larger
404 diameters than the average meteoritic nanoglobule, they still lie within the observed size range of such
405 nanoglobules (Garvie and Buseck, 2006; Nakamura-Messenger et al., 2006). Their morphologies are also
406 consistent with the smallest size fraction of experimentally produced organic globules created by UV
407 irradiation of organic molecules in ices, followed by exposure to liquid water (Dworkin et al., 2001).

408 Because only two cometary globules have so far been discovered, it is unknown if they are
409 representative of the entire population preserved in the comet. Because the capture of cometary dust in
410 aerogel is a highly energetic process (Domínguez et al., 2004), it is possible that smaller organic globules
411 with thinner walls, similar to average meteoritic nanoglobules, may be destroyed by thermal and
412 frictional forces. Alternatively, smaller globules may be more difficult to recognize when mixed with
413 melted or compressed aerogel and other materials. This would create a sampling bias towards the
414 recovery of large, thick-walled organic globules in the cometary return samples.

415 The D/H ratio measured in the Track 2 globule ($\delta D = +1000\%$) lies well outside the range of
416 terrestrial materials and is similar to that of other Wild 2 carbonaceous samples (McKeegan et al., 2006)
417 and bulk IOM residues from primitive CI and CM chondrites (Alexander et al., 2007). However, the Track
418 2 globule is less D-enriched than bulk IOM residues from primitive CR and ordinary chondrites
419 (Busemann et al., 2006; Alexander et al., 2007) and organic nanoglobules from Tagish Lake (Nakamura-
420 Messenger et al., 2006). Prior to this study, such magnitude D enrichments would have been considered
421 unambiguous evidence for an extraterrestrial origin. However, the C-XANES spectrum of this globule
422 that was acquired prior to TEM analysis is strikingly similar to cyanoacrylate adhesive. If this globule is
423 indeed a cyanoacrylate contaminant from sample preparation, exposure to electron irradiation during
424 TEM analysis could have chemically altered the organic matter and depleted it in H relative to D,
425 resulting in an effective D enrichment. We estimate that during TEM and STEM characterization the
426 Track 2 globule was exposed to a similar total electron fluence (about 10^7 electrons/nm²) as our
427 irradiated cyanoacrylate and epoxy standards. Since a comparable D enrichment was observed in those
428 irradiated adhesive samples, the D enrichment measured in the Track 2 globule could have been
429 induced during TEM analysis. A corresponding ¹⁵N enrichment, which was not produced by our electron
430 irradiation experiments, is not present in the Track 2 globule, despite it being N-rich. Despite these
431 considerations, it remains possible that the Track 2 globule is indeed cometary organic matter. Given the

432 large variations in organic chemistry that have been observed in other organic Stardust samples (Cody et
433 al., 2008a), the Track 2 globule may represent primitive nitrile and carboxyl-rich interstellar organic
434 matter. In addition, the hollow spherical morphology is not consistent with other cyanoacrylate marker
435 sections found on Stardust mounts. However, because of the similarities with cyanoacrylate, a cometary
436 origin cannot be unambiguously determined at this time. The potential future detection of other
437 Stardust globules with similar XANES spectra, along with isotopic measurements made on sections not
438 previously exposed to electron irradiation, may settle this question. Therefore, in the remainder of our
439 discussion we will focus primarily on results from the Track 80 globule.

440 In contrast to the Track 2 sample, the Track 80 globule contains a large enrichment in ^{15}N and a
441 moderate depletion in ^{13}C . Unfortunately, its hydrogen isotopic composition could not be reliably
442 determined due to substrate failure during the analysis, although our data does place an upper limit on
443 its D/H ratio (Table 1), well below the extreme D enrichments that have been observed in some
444 meteoritic nanoglobules (Ashley et al., 2005; Nakamura-Messenger et al., 2006). The ^{15}N isotopic
445 anomaly in the Track 80 globule lies significantly outside the range of terrestrial and most other solar
446 system materials (Figure 5). Kinetic fractionation during evaporation would tend to enrich the
447 condensed phase in the heavy stable isotopes. Reaching the observed $^{15}\text{N}/^{14}\text{N}$ composition in the Track
448 80 globule through a Rayleigh-like process would require extreme loss of material and simultaneously
449 lead to large ^{13}C enrichments. Since the Track 80 globule is depleted in ^{13}C , evaporation or condensation
450 cannot be responsible for these isotopic anomalies. This additionally rules out laboratory isotopic
451 enrichments generated during sample storage or preparation.

452 The $^{15}\text{N}/^{14}\text{N}$ and $^{13}\text{C}/^{12}\text{C}$ isotopic ratios observed in the Track 80 globule are remarkably similar to
453 those of two anomalous “hotspots” previously reported in Wild 2 samples (McKeegan et al., 2006), one
454 of which was located within an Al foil impact crater and one in an aerogel track sample. Although it is
455 not known whether these other samples contained nanoglobules, the isotopic similarity strongly

456 suggests that additional nanoglobules should be present in the Stardust sample collection. The isotopic
457 composition of the Track 80 globule is also very similar to carbonaceous sub-grains in primitive
458 anhydrous IDPs (Floss et al., 2004) and the CR chondrites EET 92042 (Busemann et al., 2006) and QUE
459 99177 (Floss and Stadermann, 2009). Unfortunately, the morphologies of most of these grains have not
460 been observed, reported, and/or adequately determined to ascertain whether or not they are
461 nanoglobules. Relatively few isotopic measurements have been reported for individual meteoritic
462 nanoglobules, with most of the extant data obtained from the Tagish Lake carbonaceous chondrite
463 (Ashley et al., 2005; Nakamura-Messenger et al., 2006). Nanoglobules in Tagish Lake are typically
464 enriched in ^{15}N and D, with $\delta^{15}\text{N}$ values ranging from 200‰ to 1000‰ (Nakamura-Messenger et al.,
465 2006), significantly above the bulk IOM value of $\sim 75\%$ (Grady et al., 2002; Alexander et al., 2007). On
466 the other hand, IOM from the Bells (anomalous CM2) meteorite has higher $\delta^{15}\text{N}$ values both in bulk
467 material (400‰) and in hotspots ($\leq 3200\%$; Busemann et al., 2006), at least some of which contain
468 nanoglobules (Messenger et al., 2008).

469 The Track 80 globule also bears a chemical resemblance to at least some meteoritic
470 nanoglobules. Most notably, both it and the larger nanoglobule from the Murchison residue (M1; Figure
471 1D) show very similar C-XANES spectra, indicating the presence of highly aromatic organic matter.
472 Previous analyses of nanoglobule chemistry in Murchison and other primitive meteorites by electron
473 energy-loss spectroscopy (EELS) in TEM also indicated a highly aromatic character (Garvie and Buseck,
474 2004; Garvie, 2006). However, the spectral resolution of this technique is significantly poorer than that
475 of the STXM methods used in this study, and EELS may be more destructive and less sensitive than
476 XANES for detecting particular organic functional groups, such as carboxyl or ketones (Braun et al.,
477 2005), which are common in extraterrestrial organic matter.

478 Like most of the reported carbonaceous cometary samples from the Stardust collection
479 (Sandford et al., 2006; Cody et al., 2008a), the Track 80 samples reported here have atomic N/C ratios

480 (0.10-0.15) significantly higher than those measured in bulk IOM from primitive CM, CR, and CI
481 chondrites (0.03-0.04; Alexander et al., 2007). Anhydrous IDPs, which are likely cometary in origin, also
482 contain high nitrogen abundances (Keller et al., 2004). Atomic N/C ratios were not determined for the
483 Murchison globules in this study. EELS measurements performed by Garvie and Buseck (2004) did
484 provide chemical compositions for several meteoritic nanoglobules. Most of these had N/C ratios in the
485 range of bulk IOM. However, a few did show higher nitrogen abundances, with N/C as high as 0.10-0.16
486 in nanoglobules from Tagish Lake (C-ungrouped) and Cold Bokkeveld (CM2), similar to that observed in
487 the Wild 2 samples.

488 Taken together, the results from the Track 80 organic section and the Track 80 globule
489 demonstrate that comets contain very similar organic solids to chondrites. Morphologically, chemically,
490 and isotopically, the Stardust Track 80 globule resembles at least one class of the nanoglobules found in
491 meteorites and IDPs, whereas the Track 80 organic section is morphologically, isotopically, and
492 chemically similar to non-globular IOM in meteorites. Both IOM-like carbonaceous matter and organic
493 nanoglobules appear to be ubiquitous in the Solar System and were sampled by comets and primitive
494 meteorites during their accretionary phases.

495

496

497 **4.2. Organic globule formation**

498 Although various mechanisms have been proposed to explain the formation of organic
499 nanoglobules, most rely on one of three general methods: (i) processes that occur in circumstellar
500 environments, (ii) interaction with interstellar or nebular ice in extremely cold environments, or (iii)
501 aqueous processes on parent bodies. Spherical presolar graphites and SiC grains with highly anomalous
502 C isotopic compositions have been observed in several meteoritic acid residues and are believed to have
503 formed in the circumstellar envelopes of asymptotic giant branch stars or within expanding supernova

504 ejecta (Bernatowicz et al., 1996; Nittler, 2003; Croat et al., 2005). Recently, organic globules have been
505 synthesized from simple aromatic molecules exposed to helium plasma, suggesting that such objects
506 could form from PAHs around evolved stars or possibly within the primitive solar nebula (Saito and
507 Kimura, 2009). Presolar graphites range in size from 250 nm to tens of μm (Croat et al., 2005), generally
508 larger than that observed for meteoritic nanoglobules (Garvie and Buseck, 2006; Nakamura-Messenger
509 et al., 2006), but consistent with the cometary globules described here. However, the plasma-generated
510 globules had diameters of less than 150 nm (Saito and Kimura, 2009), much smaller than most
511 meteoritic nanoglobules and the cometary globules. Presolar graphite and SiC grains have C and N
512 isotopic ratios that span several orders of magnitude, including rare grains, thought to originate in
513 supernovae, with ^{15}N enrichments and relatively close-to-solar $^{12}\text{C}/^{13}\text{C}$ ratios, as observed in the Track 80
514 globule. Thus, strictly speaking, an origin as a supernova condensate cannot be ruled out. However, the
515 rarity of such compositions in the general presolar grain population and the similarity of the Track 80
516 globule composition to other ^{15}N isotopic hotspots in extraterrestrial samples argue against a
517 circumstellar origin for this globule.

518 Organic nanoglobules in the Tagish Lake and Bells carbonaceous chondrites have been
519 hypothesized to form from organic molecules in ice grains in the interstellar medium or outer solar
520 nebula (Nakamura-Messenger et al., 2006; Messenger et al., 2008). In this model, ion-molecule
521 reactions enrich organics on the surface of ice grains in ^{15}N and/or D while simultaneously generating a
522 coherent surface coating through the gradual accumulation of organic matter and the generation of
523 more refractory organic matter by UV irradiation. At some point, the ice is removed through sublimation
524 or melting, leaving a hollow spherical globule. Radiation processing may accelerate both ice removal and
525 the formation of increasingly refractory organic matter, eventually resulting in impermeable
526 nanoglobules. Afterwards, the hollow nanoglobules are transported throughout the protostellar disk as
527 discrete grains, which may eventually be incorporated into comets, asteroids, and IDPs.

528 The highly aromatic nature of the Track 80 globule indicates that it formed from PAH-like or
529 other refractory organic precursors, which is consistent with the formation model proposed for the
530 Tagish Lake nanoglobules (Nakamura-Messenger et al., 2006). However, the Tagish Lake globules also
531 appear to contain aliphatic and oxygenated functional group chemistry (Nakamura et al., 2003), which
532 has not been observed in the Track 80 globule. In fact, a wide variety of chemical functionality may be
533 produced by ion-molecule reactions on ice grains, which might be expected to result in chemically
534 heterogeneous nanoglobules. Similarly, D/H and $^{15}\text{N}/^{14}\text{N}$ fractionation may proceed via several reaction
535 pathways depending on which organic molecules/ions are present (as described below), resulting in
536 varied levels of isotopic enrichment. In general, however, significant D enrichments should be present in
537 organic matter that formed in cold extraterrestrial environments. Based on these assumptions, the
538 homogeneous aromatic chemistry and the lack of a significant D enrichment in the Track 80 globule
539 suggest either that it did not form by these mechanisms or that its chemistry and isotopic composition
540 have been significantly altered following its formation.

541 If transient aqueous fluids were present on Comet Wild 2, then organic globules may have
542 formed by interaction with water. Experimental irradiation of interstellar analogue ices with UV light has
543 been shown to synthesize amphipathic molecules, which may form organic vesicles when the ice melts
544 (Dworkin et al., 2001). The amphipathic molecules created during these experiments require the initial
545 presence of methanol in the ice, but other alcohols or carboxylic acid will likely perform the same
546 function. In this model, liquid water must be present at some time so that the amphipathic molecules
547 can arrange themselves into globules and vesicles. Evidence of aqueous parent body processing is
548 common in meteorites, and laboratory-produced, spherical, carbonaceous grains have been generated
549 during hydrothermal processing of meteoritic IOM analog materials (Cody et al., 2009). However,
550 aqueous fluids are not expected to be abundant on cometary bodies. Localized heating may occur on
551 the comet during accretion or mass-redistribution events, which can temporarily generate small pockets

552 of liquid water. Transient heating may also occur during shock events involving interstellar or
553 protostellar ice, although such events would be more prevalent in dense stellar cores or during initial
554 star formation. In these vacuum environments, however, water-ice is expected to sublime rather than
555 melt. If liquid water does result from grain-grain collisions or shock wave events (Ciesla et al., 2003),
556 then organic globule morphology could be formed in the protosolar nebula, even though most of the
557 isotopic fractionation occurred in the molecular cloud.

558 Capture of cometary ices in Stardust aerogel is another transient heating process (Domínguez et
559 al., 2004; Noguchi et al., 2007), which may, in principle, result in nanoglobule formation. Captured ice
560 grains would have volatilized quickly (on the order of several microseconds), so any globule
561 morphologies created by this process should have formed extremely quickly from small amounts of
562 liquid water. Globules formed at the time of capture would be expected to have similar organic
563 chemistry and functionality to nearby non-globular cometary organic matter. An exception to this rule
564 could be made for labile organic molecules that are substantially more amphipathic than the remaining
565 organic matter. Amphipathic organic molecules would contain polar terminal functional groups such as
566 alcohol (C-OH), carbonyl (C=O), and nitrile (C≡N). Although polycyclic aromatic hydrocarbons are
567 typically non-polar, carbon atoms at the edges of ring structures can be modified with polar functional
568 groups. If present in interstellar globules, these polar functional groups should be observable by XANES,
569 as they are in the Track 2 globule.

570 The organic composition of the Track 80 globule indicates that it probably did not form during
571 transient heating of interstellar ices or particle capture. Although it and the associated Track 80 organic
572 section are both enriched in ¹⁵N, the organic functionality of the globule is very distinct from that of the
573 other cometary organic matter and, due to its highly aromatic nature, the organic matter in the globule
574 is significantly less amphipathic than the latter. Since a more amphipathic and more polar organic
575 fraction would be expected to be extracted from cometary organic matter and form globule-like

576 morphologies during transient heating events, the highly aromatic Track 80 globule could not have
577 formed via this process and most likely did not form during particle capture. Similarly, it is not likely that
578 the globule formed out of amphipathic organics generated by UV photolysis. Rather, the Track 80
579 globule morphology was present in comet Wild 2 prior to capture by the Stardust spacecraft.

580 It is possible that the highly aromatic chemistry observed in the Track 80 globule is a post-
581 formation processing signature of exposure to high-energy nebular or interstellar environments. As
582 observed in the Track 2 globule, after extensive damage during TEM analysis with 200 keV electrons,
583 aromatic carbon may be created and other functional groups may be destroyed by radiation processing.
584 It may be possible, then, that exposure to high-energy ionizing radiation for long periods of time may
585 aromatize a complex aliphatic nanoglobule, which would also likely alter its D/H composition. This
586 process is distinct from direct “knock-on” damage from ion bombardment, which leads to significant loss
587 of N and O, producing elemental amorphous carbon (Strazzulla and Baratta, 1992). Amorphized organic
588 matter from irradiation has been reported in primitive chondrites (Busemann et al., 2007) and Wild 2
589 carbonaceous samples (Rotundi et al., 2008). Highly aromatic globules may indicate significant exposure
590 to galactic cosmic rays, which typically include a few percent of high-energy electrons (Yoshida, 2008), or
591 to energetic electrons in solar wind and other solar mass outflows.

592 Observed fluxes of high-energy electrons from such sources can be compared to the electron
593 fluence to which the Track 2 globule was exposed during TEM analysis ($\sim 10^7$ electrons/nm²), which had
594 completely altered its organic chemistry. It should be noted, however, that significant chemical change
595 may be induced in organic samples exposed to far less fluence (likely as little as 10^5 electrons/nm²).
596 Unfortunately, galactic cosmic ray electrons with energies that are most likely to affect chemical change
597 in 1-2 μ m organic particles (between 1 keV and 1 MeV) are difficult to observe directly, since such
598 electrons with energies less than 1 GeV are modulated by the solar heliosphere (Yoshida, 2008). Within
599 the interstellar medium, extrapolations of the observed cosmic ray electron flux spectrum to lower

600 energies are poorly constrained (Strong et al., 2000), and the total inferred electron flux can range from
601 10^{-1} - 10^5 electrons/cm² per second, based on the model chosen (Padovani et al., 2009). Based on these
602 electron fluxes, it would take anywhere from 10^7 - 10^{15} years to achieve a comparable electron fluence to
603 which the Track 2 globule was exposed during TEM. Within the solar nebula, fast solar wind electrons
604 with energies between 1 keV and 1 MeV can be measured by various instruments on the WIND and
605 STEREO spacecrafts, indicating total electron fluxes on the order of 10^5 electrons/cm² per second at 1
606 AU (Lin et al., 1995, 2008). This value suggests that it would take about 10^7 - 10^9 years to match the
607 electron fluence to which the Track 2 globule was exposed during TEM. Although this residence time in
608 the solar nebula is too long to complete the irradiation before accretion onto comet or asteroid parent
609 bodies (Nichols, 2006), there are many factors which may reduce this time. The solar wind flux has a
610 $1/R^2$ dependence away from the Sun, which would require organic globules to be present in the inner
611 regions of the nebula during this time. Secondly, the particle flux from the early Sun could have been as
612 much as 1000 times larger than it is today (Wood et al., 2002), and events such as solar flares and
613 coronal mass ejections can increase the flux of high-energy electrons by several orders of magnitude (Lin
614 and Hudson, 1976; Simnett et al., 2002). Although our estimates are currently poorly constrained, we
615 find it reasonable that the original organic chemistry of nanoglobules could be significantly altered by
616 energetic electrons on achievable timescales in both the interstellar medium and within the solar
617 nebula. This may provide a novel and relevant mechanism for both the formation of PAHs and D-
618 enrichments in molecular clouds.

619

620 **4.3. Interstellar cloud chemistry**

621 Ion-molecule and gas-grain interactions in extremely cold interstellar environments can result in
622 large isotopic fractionation of H and N, although there are many conditions under which D may be
623 significantly enriched without a simultaneous ¹⁵N enrichment (Herbst, 2003). Although organic matter in

624 IDPs and primitive meteorites is typically enriched in both D and ^{15}N , the enrichments are largely
625 decoupled at the microscale, with the largest D and ^{15}N enrichments localized in distinct isotopic
626 hotspots (Robert and Epstein, 1982; Keller et al., 2004; Busemann et al., 2006). Nonetheless, ^{15}N
627 hotspots in these samples are generally somewhat D-rich, in contrast to the Track 80 cometary globule,
628 in which the ^{15}N enrichment is present without a corresponding D anomaly (although, as mentioned
629 above, we cannot rule out a modest D enrichment due failure of the support film during the D/H
630 measurement). This observation may indicate either that there are conditions under which N isotopic
631 fractionation occurs without H isotopic fractionation, or that the D-enrichments are removed by
632 subsequent processing.

633 Current models of nitrogen isotopic fractionation depend on the selective depletion or freezing
634 out of carbon monoxide and alcohols in dense molecular cloud cores in order to reach ^{15}N enrichments
635 observed in the Track 80 globule (Charnley and Rodgers, 2002). In the presence of gaseous CO, the ^{15}N
636 enrichment factor cannot exceed about 1.3 above terrestrial values in the standard molecular cloud
637 model (Terzieva and Herbst, 2000). In interstellar clouds, ^{15}N fractionation up to +10,000‰ can occur at
638 low temperatures around 10 K in ammonia ice mantles (Rodgers and Charnley, 2008a), but is less than
639 +4,000‰ for nitrogen heterocycles in PAHs (Rodgers and Charnley, 2004) or nitrile functional groups
640 (Rodgers and Charnley, 2008b) adsorbed onto icy grains. Astronomical observations of CN in comets
641 (Schulz et al., 2008) suggest that nitrile functional groups may be the carriers of presolar ^{15}N , and ^{15}N
642 enrichments in IDPs appear to be associated with amine (C-NH_x) bonds (Keller et al., 2004). However,
643 given that the organic matter in the Track 80 globule is predominantly aromatic and lacks evidence of
644 abundant nitrile or amine functionality, PAHs appear to be the carrier of anomalous ^{15}N . Unfortunately,
645 N-XANES was not performed on this globule prior to NanoSIMS analysis to confirm the presence of
646 nitrogen heterocycles, such as pyridine or pyrrole, which have nitrogen photoabsorptions at 398.8 eV
647 and 402.2 eV. Due to the diversity of observed and implied organic carriers of anomalous ^{15}N , many

648 fractionation mechanisms may regularly occur in dark molecular clouds or the outer cold regions of the
649 solar nebula.

650 Models of D isotopic fractionation indicate that it is also strongly dependent on temperature,
651 and large isotopic anomalies may be generated by ion-molecule reactions in interstellar gases with
652 temperatures up to 70 K (Millar et al., 1989). Similar deuterating reactions may also occur in collapsing
653 protoplanetary disks as close in as 30 astronomical units from the central star (Aikawa and Herbst, 1999)
654 in the region of the Kuiper belt where many comets and icy bodies accumulate. Organic molecules
655 adsorbed to the surface of ice and dust grains may become D-enriched through gas-grain interactions
656 (Tielens, 1983). Deuterated primary molecules within ice grains will be transformed into reactive species
657 during UV photolysis, propagating the D enrichment to larger organic molecules (Sandford et al., 2000,
658 2001), which may then be released as isotopically-anomalous organic particles within the molecular
659 cloud or solar nebula. Gas phase D enrichments can be enhanced by selective depletion of CO (Bacmann
660 et al., 2003), which is required for large ^{15}N enrichments. In selectively depleted cold environments,
661 both ^{15}N and D may be enriched simultaneously, producing organic molecules or globules with
662 anomalies in both isotopes, such as those observed in globules from carbonaceous chondrites and IDPs
663 (Nakamura-Messenger et al., 2006; Messenger et al., 2008).

664 As indicated by TEM-based irradiation of cyanoacrylate and epoxy by 200 keV electrons,
665 significant D-enrichments may be generated in extraterrestrial organic matter by long term exposure to
666 high-energy electrons. Such enrichments may occur in warmer regions of the interstellar medium and
667 do not require the specific molecular cloud compositions necessary for ion-molecule or gas-grain
668 isotopic fractionation mechanisms. The estimated residence times (perhaps as little as 10 million years)
669 necessary to produce significant chemical and isotopic changes in interstellar organic matter suggest
670 that electron radiolysis is a potentially important mechanism in molecular clouds. This process would be
671 likely to be much less effective within much of the solar nebula except for the innermost regions, where

672 the electron flux is similar to that of cosmic rays in the interstellar medium. However likely this
673 mechanism of D fractionation may be, the potential for D-enrichment from electron irradiation should
674 be considered in future interpretations of extreme D enrichments in meteorites and other planetary
675 materials.

676 In PAHs and PAH-like organic molecules, ^{15}N atoms will be primarily located in heteroatomic,
677 aromatic moieties, while D atoms are attached to the edges of polyaromatic domains. Due to the
678 relative stability of nitrogen in heteroatomic sites, the ^{15}N enrichment of PAHs should not change much
679 over time. Conversely, hydrogen and D atoms on the edges of PAHs may be exchanged relatively easily
680 by a variety of mechanisms, including exposure to UV radiation within the solar nebula (Sandford et al.,
681 2001). If D-rich organic matter is not protected within cometary bodies or other planetesimals, it is
682 possible that UV-driven hydrogen exchange could drive the D/H ratio back towards solar abundances or
683 the average isotopic composition of the local nebular environment. Closer to the proto-star, D/H may be
684 steadily increased by interactions with high-energy solar wind electrons, although the rate of D-
685 enrichment via this mechanism is likely slower than isotopic re-equilibration by UV-irradiation. Similarly,
686 exposure to aqueous fluids on a parent body may also re-equilibrate the hydrogen isotopic composition
687 of an organic globule without affecting its nitrogen composition. The isotopic composition observed in
688 the Track 80 globule may be a result of such processes.

689

690

5. CONCLUSIONS

691 Organic nanoglobules containing D and/or ^{15}N isotopic anomalies appear to have been
692 widespread in the early solar system. At least one of the two hollow organic globules described herein
693 was once a component of comet 81P/Wild 2, as revealed by its isotopic composition and association
694 with aerogel from the Stardust collector tray, and is the first authentic organic globule reported in
695 cometary samples. The Track 80 globule, composed of highly aromatic PAH-like organic matter, contains

696 a ^{15}N enrichment that is similar to other Wild 2 isotopic hotspots and anomalous grains in primitive IDPs
697 and chondrites, which also likely include some nanoglobules. The similarity in chemistry and nitrogen
698 isotopic composition to a globule from the Murchison meteorite indicates that Wild 2 and the
699 Murchison parent body sampled similar reservoirs of primitive organic matter in the early Solar nebula.
700 However, the N/C ratio of this cometary globule (0.10-0.15), like other carbonaceous Stardust samples,
701 is significantly higher than typical meteoritic organic matter, suggesting that the organic matter
702 composing the Track 80 globule is some of the most primitive in our Solar System. In contrast, the
703 presence of a D enrichment, but isotopically normal nitrogen composition, in the Track 2 globule means
704 that a cometary origin cannot be definitively determined. Instead, it likely represents a cyanoacrylate
705 contaminant with a D enrichment resulting from electron irradiation during TEM analysis. We have
706 demonstrated that relative D enrichments of 1000‰ can be induced in ultramicrotome sections of
707 common organic adhesives during typical TEM analyses of Stardust samples, creating ambiguity for the
708 interpretation of potentially interstellar organic matter that has been observed with TEM prior to
709 measuring its isotopic composition. This experimental result also indicates that electrons with energies
710 between $10^3 - 10^6$ eV may play an important role in processing and deuterating organic molecules in the
711 extraterrestrial environments.

712 At present, there is no model of the formation and processing history of organic nanoglobules
713 that fully explains the range of observed morphologies, chemistries, and isotopic compositions. The
714 widespread occurrence of globules in diverse parent bodies could reflect either their prevalence
715 throughout the protosolar molecular cloud prior to its collapse, or formation in the solar nebula by a
716 common process from a common set of precursors, perhaps followed by large-scale material transport
717 (e.g. Ciesla, 2007). The anomalous abundances of ^{15}N and/or D preserved in these globules suggest
718 isotopic fractionation in cold molecular clouds, although fractionation in the outer regions of the
719 protosolar nebula cannot be ruled out.

720 The cometary Track 80 globule is highly enriched in ^{15}N and slightly depleted in ^{13}C , but appears
721 to lack a correlated large D enrichment. This decoupling of ^{15}N and D enrichments could have occurred
722 at the time of formation as a result of the molecular composition of the environment, or through
723 subsequent processing events, including radiation exposure or aqueous alteration. One possible origin
724 for the Track 80 globule is within a cold ($\sim 10\text{ K}$), dense, molecular cloud core where PAHs were prevalent,
725 but carbon monoxide had been selectively depleted. The ^{15}N enrichment of organic matter in such an
726 interstellar environment could be increased if PAHs were present on the surface of ice grains. Exposure
727 to cosmic ray electrons may have aromatized the organic matter on the surface and volatilized the
728 internal ice grain, leaving a hollow organic globule. Alternatively, the organic matter in a fully-formed
729 globule may have been aromatized by residence in the inner regions of the nebula. Irradiation of the
730 globule by UV photons while in the relatively warm nebula may also have led to isotopic re-
731 equilibration of D/H towards typical solar values without affecting the ^{15}N protected in stable
732 heteroatomic aromatic moieties. Due to the highly aromatic nature of the Track 80 globule, its
733 morphology is most likely not a result of exposure to transient aqueous fluids on the cometary parent
734 body, although such exposure may also serve to re-equilibrate its D composition.

735
736 *Acknowledgements.* The authors gratefully acknowledge the support of Sue Wirick, Nabil Bassim, and
737 Dominic Papineau with the acquisition of STXM data. Additional thoughtful discussion was provided by
738 George Cody. We also sincerely thank the reviewers, Gary Huss, Frank Stadermann, and Laurence
739 Garvie, whose criticisms and suggestions significantly improved the article's content and clarity. Use of
740 the Advanced Light Source and the National Synchrotron Light Source was supported by the U.S.
741 Department of Energy. Financial support for this research came from the Office of Naval Research, NASA
742 Discovery Data Analysis and Origins of Solar Systems Program, and NASA Astrobiology Institute. This

743 research was conducted while the primary author held a National Research Council Research
744 Associateship at the U.S. Naval Research Laboratory.

745

746

747 REFERENCES

- 748 Ade H. and Urquhart S. G. (2002) NEXAFS spectroscopy and microscopy of natural and synthetic
749 polymers. In: *Chemical Applications of Synchrotron Radiation* (ed. T. Sham), *Adv. Ser. Phys.*
750 *Chem.* **1**. World Scientific, Singapore. pp. 285-355.
- 751 Ahuja R., Brühwiler P. A., Wills J. M., Johansson B., Mårtensson N. and Eriksson O. (1996) Theoretical and
752 experimental study of the graphite 1s x-ray absorption edges. *Phys. Rev. B* **54**, 14396-14404.
- 753 Aikawa Y. and Herbst E. (1999) Deuterium fractionation in protoplanetary disks. *Astrophys. J.* **526**, 314-
754 326.
- 755 Alexander C. M. O'D., Fogel M., Yabuta H. and Cody G. D. (2007) The origin and evolution of chondrites
756 recorded in the elemental and isotopic compositions of their macromolecular organic matter.
757 *Geochim. Cosmochim. Acta* **71**, 4380-4403.
- 758 Alexander C. M. O'D., Russell S. S., Arden J. W., Ash R. D., Grady M. M. and Pillinger C. T. (1998) The
759 origin of chondritic macromolecular organic matter: A carbon and nitrogen isotope study.
760 *Meteorit. Planet. Sci.* **33**, 603-622.
- 761 Apen E., Hitchcock A. P. and Gland J. L. (1993) Experimental studies of the core excitation of imidazole,
762 4, 5-dicyanoimidazole, and s-triazine. *J. Phys. Chem.* **97**, 6859-6866.
- 763 Ashley J. W., Huss G. R., Garvie L. A. J., Guan Y., Buseck P. R. and Williams L. B. (2005) Nitrogen and
764 carbon isotopic measurements of carbon nanoglobules from the Tagish Lake meteorite by
765 secondary ion mass spectrometry. In: *Lunar Planet. Sci. XXXIV*. Lunar Planet. Inst., Houston, TX.
766 #2205 (abstr.).
- 767 Bacmann A., Lefloch B., Ceccarelli C., Steinacker J., Castets A. and Loinard L. (2003) CO depletion and
768 deuterium fractionation in prestellar cores. *Astrophys. J. Lett.* **585**, L55-L58.

769 Belavin V. V., Okotrub A. V., Bulusheva L. G., Kotosonov A. S., Vyalykh D. V. and Molodtsov S. L. (2006)
770 Determining misorientation of graphite grains from the angular dependence of X-ray emission
771 spectra. *J. Exp. Theor. Phys.* **103**, 604-610.

772 Bernatowicz T. J., Cowsik R., Gibbons P. C., Lodders K., Fegley B. Jr., Amari S. and Lewis R. S. (1996)
773 Constraints on stellar grain formation from presolar graphite in the Murchison meteorite.
774 *Astrophys. J.* **472**, 760-782.

775 Boyce C. K., Cody G. D., Feser M., Jacobsen C., Knoll A. H. and Wirick S. (2002) Organic chemical
776 differentiation within fossil plant cell walls detected with X-ray spectromicroscopy. *Geology* **30**,
777 1039-1042.

778 Braun A., Huggins F. E., Shah N., Chen Y., Wirick S., Mun S. B., Jacobsen C. and Huffman G. P. (2005)
779 Advantages of soft X-ray absorption over TEM-EELS for solid carbon studies--a comparative
780 study on diesel soot with EELS and NEXAFS. *Carbon* **43**, 117-124.

781 Brownlee D. E., Tsou P., Aleon J., Alexander C. M. O., Araki T., Bajt S., Baratta G. A., Bastien R., Bland P.,
782 Bleuet P., Borg J., Bradley J. P., Brearley A., Brenker F., Brennan S., Bridges J. C., Browning N. D.,
783 Brucato J. R., Bullock E., Burchell M. J., Busemann H., Butterworth A., Chaussidon M., Cheuvront
784 A., Chi M., Cintala M. J., Clark B. C., Clemett S. J., Cody G., Colangeli L., Cooper G., Cordier P.,
785 Daghlian C., Dai Z., D'Hendecourt L., Djouadi Z., Dominguez G., Duxbury T., Dworkin J. P., Ebel D.
786 S., Economou T. E., Fakra S., Fairey S. A. J., Fallon S., Ferrini G., Ferroir T., Fleckenstein H., Floss
787 C., Flynn G., Franchi I. A., Fries M., Gainsforth Z., Gallien J., Genge M., Gilles M. K., Gillet P.,
788 Gilmour J., Glavin D. P., Gounelle M., Grady M. M., Graham G. A., Grant P. G., Green S. F.,
789 Grossemy F., Grossman L., Grossman J. N., Guan Y., Hagiya K., Harvey R., Heck P., Herzog G. F.,
790 Hoppe P., Horz F., Huth J., Hutcheon I. D., Ignatyev K., Ishii H., Ito M., Jacob D., Jacobsen C.,
791 Jacobsen S., Jones S., Joswiak D., Jurewicz A., Kearsley A. T., Keller L. P., Khodja H., Kilcoyne A. D.,
792 Kissel J., Krot A., Langenhorst F., Lanzirotti A., Le L., Leshin L. A., Leitner J., Lemelle L., Leroux H.,

793 Liu M., Luening K., Lyon I., MacPherson G., Marcus M. A., Marhas K., Marty B., Matrajt G.,
794 McKeegan K., Meibom A., Mennella V., Messenger K., Messenger S., Mikouchi T., Mostefaoui S.,
795 Nakamura T., Nakano T., Newville M., Nittler L. R., Ohnishi I., Ohsumi K., Okudaira K.,
796 Papanastassiou D. A., Palma R., Palumbo M. E., Pepin R. O., Perkins D., Perronnet M., Pianetta
797 P., Rao W., Rietmeijer F. J. M., Robert F., Rost D., Rotundi A., Ryan R., Sandford S. A., Schwandt
798 C. S., See T. H., Schlutter D., Sheffield-Parker J., Simionovici A., Simon S., Sitnitsky I., Snead C. J.,
799 Spencer M. K., Stadermann F. J., Steele A., Stephan T., Stroud R., Susini J., Sutton S. R., Suzuki Y.,
800 Taheri M., Taylor S., Teslich N., Tomeoka K., Tomioka N., Toppani A., Trigo-Rodriguez J. M.,
801 Troadec D., Tsuchiyama A., Tuzzolino A. J., Tyliczszak T., Uesugi K., Velbel M., Vellenga J., Vicenzi
802 E., Vincze L., Warren J., Weber I., Weisberg M., Westphal A. J., Wirick S., Wooden D., Wopenka
803 B., Wozniakiewicz P., Wright I., Yabuta H., Yano H., Young E. D., Zare R. N., Zega T., Ziegler K.,
804 Zimmerman L., Zinner E. and Zolensky M. (2006) Comet 81P/Wild 2 under a microscope. *Science*
805 **314**, 1711-1716.

806 Brühwiler P. A., Maxwell A. J., Puglia C., Nilsson A., Anderson S. and Mårtensson N. (1995) π^* and σ^*
807 excitons in C 1s absorption of graphite. *Phys. Rev. Lett.* **74**, 614-617.

808 Busemann H., Alexander C. M. O'D. and Nittler L. R. (2007) Characterization of insoluble organic matter
809 in primitive meteorites by microRaman spectroscopy. *Meteorit. Planet. Sci.* **42**, 1387-1416.

810 Busemann H., Nguyen A. N., Cody G. D., Hoppe P., Kilcoyne A. L. D., Stroud R. M., Zega T. J. and Nittler L.
811 R. (2009) Ultra-primitive interplanetary dust particles from the comet 26P/Grigg-Skjellerup dust
812 stream collection. *Earth Planet. Sci. Lett.* **288**, 44-57.

813 Busemann H., Young A. F., Alexander C. M. O'D., Hoppe P., Mukhopadhyay S. and Nittler L. R. (2006)
814 Interstellar chemistry recorded in organic matter from primitive meteorites. *Science* **312**, 727-
815 730.

816 Charnley S. B. and Rodgers S. D. (2002) The end of interstellar chemistry as the origin of nitrogen in
817 comets and meteorites. *Astrophys. J. Lett.* **569**, L133-L137.

818 Ciesla F. J. (2007) Outward transport of high-temperature materials around the midplane of the solar
819 nebula. *Science* **318**, 613-615.

820 Ciesla F. J., Lauretta D. S., Cohen B. A. and Hood, L. L. (2003) A nebular origin for chondritic fine-grained
821 phyllosilicates. *Science* **299**, 549-552.

822 Cody G. D. (2000) Probing chemistry within the membrane structure of wood with soft X-ray spectral
823 microscopy. In: *X-Ray Microscopy* (eds. T. Warwick, W. Meyer-Ilse and D. Attwood), *AIP Conf.*
824 *Proc.* **507**. American Inst. Phys., Melville, NY. pp. 307-312.

825 Cody G. D., Ade H., Alexander C. M. O'D., Araki T., Butterworth A. L., Fleckenstein H., Flynn G. J., Gilles
826 M. K., Jacobsen C., Kilcoyne A. L. D., Messenger K., Sandford S. A., Tyliszczak T., Westphal A. J.,
827 Wirick S. and Yabuta H. (2008a) Quantitative organic and light-element analysis of comet
828 81P/Wild 2 particles using C-, N-, and O- μ -XANES. *Meteorit. Planet. Sci.* **43**, 353-365.

829 Cody G. D. and Alexander C. M. O'D. (2005) NMR studies of chemical structural variation of insoluble
830 organic matter from different carbonaceous chondrite groups. *Geochim. Cosmochim. Acta* **69**,
831 1085-1097.

832 Cody G. D., Alexander C. M. O'D., Yabuta H., Kilcoyne A. L. D., Araki T., Ade H., Dera P., Fogel M., Militzer
833 B. and Mysen B. O. (2008b) Organic thermometry for chondritic parent bodies. *Earth Planet. Sci.*
834 *Lett.* **272**, 446-455.

835 Cody G. D., Heying E. and Alexander C. M. O'D. (2009) A post accretionary origin for meteoritic and
836 cometary organic solids? In: *Lunar Planet. Sci. XL*. Lunar Planet. Inst., The Woodlands, TX. #2325
837 (abstr.).

838 Cooper G., Gordon M., Tulumello D., Turci C., Kaznatcheev K. and Hitchcock A. P. (2004) Inner shell
839 excitation of glycine, glycyglycine, alanine and phenylalanine. *J. Electron Spectrosc. Relat.*
840 *Phenom.* **137-140**, 795-799.

841 Croat T. K., Stadermann F. J. and Bernatowicz T. J. (2005) Presolar graphite from AGB stars:
842 Microstructure and s-process enrichment. *Astrophys. J.* 631, 976-987.

843 Domínguez G., Westphal A. J., Jones S. M. and Phillips M. L. (2004) Energy loss and impact cratering in
844 aerogels: theory and experiment. *Icarus* **172**, 613-624.

845 Dworkin J. P., Deamer D. W., Sandford S. A. and Allamandola L. J. (2001) Self-assembling amphiphilic
846 molecules: Synthesis in simulated interstellar/precometary ices. *Proc. Nat. Acad. Sci. USA* **98**,
847 815-819.

848 Floss C. and Stadermann F. J. (2009) High abundance of circumstellar and interstellar C-anomalous
849 phases in the primitive CR3 chondrites QUE 99177 and MET 00426. *Astrophys. J.* **697**, 1242-
850 1255.

851 Floss C., Stadermann F. J., Bradley J., Dai Z. R., Bajt S. and Graham G. (2004) Carbon and nitrogen
852 isotopic anomalies in an anhydrous interplanetary dust particle. *Science* **303**, 1355-1358.

853 Gago R., Jiménez I. and Albella J. M. (2001) Detecting with X-ray absorption spectroscopy the
854 modifications of the bonding structure of graphitic carbon by amorphisation, hydrogenation and
855 nitrogenation. *Surf. Sci.* **482-485**, 530-536.

856 Garvie L. A. J. (2006) Extraterrestrial carbon nanospheres. *Carbon* **44**, 158-160.

857 Garvie L. A. J. and Buseck P. R. (2004) Nanosized carbon-rich grains in carbonaceous chondrite
858 meteorites. *Earth Planet. Sci. Lett.* **224**, 431-439.

859 Garvie L. A. J. and Buseck P. R. (2006) Carbonaceous materials in the acid residue from the Orgueil
860 carbonaceous chondrite meteorite. *Meteorit. Planet. Sci.* **41**, 633-642.

861 Glavin D. P., Dworkin J. P. and Sandford S. A. (2008) Detection of cometary amines in samples returned
862 by Stardust. *Meteorit. Planet. Sci.* **43**, 399-413.

863 Gordon M. L., Cooper G., Morin C., Araki T., Turci C. C., Kaznatcheyev K. and Hitchcock A. P. (2003) Inner-
864 shell excitation spectroscopy of the peptide bond: Comparison of the C 1s, N 1s, and O 1s
865 spectra of glycine, glycyL-glycine, and glycyL-glycyl-glycine. *J. Phys. Chem. A* **107**, 6144-6159.

866 Grady M. M., Verchovsky A. B., Franchi I. A., Wright I. P. and Pillinger C. T. (2002) Light element
867 geochemistry of the Tagish Lake CI2 chondrite: Comparison with CI1 and CM2 meteorites.
868 *Meteorit. Planet. Sci.* **37**, 713-735.

869 Herbst E. (2003) Isotopic fractionation by ion-molecule reactions. *Space Sci. Rev.* **106**, 293-304.

870 Hitchcock A. P., Koprinarov I., Tyliczszak T., Rightor E. G., Mitchell G. E., Dineen M. T., Hayes F., Lidy W.,
871 Priester R. D., Urquhart S. G., Smith A. P. and Ade H. (2001) Optimization of scanning
872 transmission X-ray microscopy for the identification and quantitation of reinforcing particles in
873 polyurethanes. *Ultramicrosc.* **88**, 33-49.

874 Hitchcock A. P., Urquhart S. G. and Rightor E. G. (1992) Inner-shell spectroscopy of benzaldehyde,
875 terephthalaldehyde, ethyl benzoate, terephthaloyl chloride, and phosgene: Models for core
876 excitation of poly(ethylene terephthalate). *J. Phys. Chem.* **96**, 8736-8750.

877 Jacobsen C., Wirick S., Flynn G. J. and Zimba C. (2000) Soft X-ray spectroscopy from image sequences
878 with sub-100 nm spatial resolution. *J. Microsc.* **197**, 173-184.

879 Jokic A., Schulten H., Cutler J. N., Schnitzer M. and Huang P. M. (2004) A significant abiotic pathway for
880 the formation of unknown nitrogen in nature. *Geophys. Res. Lett.* **31**, L05502.

881 Keller L. P., Messenger S., Flynn G. J., Clemett S., Wirick S. and Jacobsen C. (2004) The nature of
882 molecular cloud material in interplanetary dust. *Geochim. Cosmochim. Acta* **68**, 2577-2589.

883 Kilcoyne A. L. D., Tyliczszak T., Steele W. F., Fakra S., Hitchcock P., Franck K., Anderson E., Harteneck B.,
884 Rightor E. G., Mitchell, G. E., Hitchcock A. P., Yang L., Warwick T. and Ade H. (2003)

885 Interferometer-controlled scanning transmission X-ray microscopes at the Advanced Light
886 Source. *J. Synchrotron Radiat.* **10**, 125-136.

887 Leinweber P., Kruse J., Walley F. L., Gillespie A., Eckhardt K., Blyth R. I. R. and Regier T. (2007) Nitrogen K-
888 edge XANES--an overview of reference compounds used to identify 'unknown' organic nitrogen
889 in environmental samples. *J. Synchrotron Radiat.* **14**, 500-511.

890 Lerotic M., Jacobsen C., Schäfer T. and Vogt S. (2004) Cluster analysis of soft X-ray spectromicroscopy
891 data. *Ultramicrosc.* **100**, 35-57.

892 Lin R. P., Anderson K. A., Ashford S., Carlson C., Curtis D. W., Ergun R., Larson D. E., McFadden J.,
893 McCarthy M., Parks G. K., Rème H., Bosqued J. M., Coutelier J., Cotin F., D'Uston C., Wenzel K.-P.,
894 Sanderson T. R., Henrion J., Ronnet J. C. and Paschmann G. (1995) A three-dimensional plasma
895 and energetic particle investigation for the WIND spacecraft. *Space Sci. Rev.* **71**, 125-153.

896 Lin R. P., Curtis D. W., Larson D. E., Luhmann J. G., McBride S. E., Maier M. R., Moreau T., Tindall C. S.,
897 Turin P. and Wang L. (2008) The STEREO IMPACT suprathermal electron (STE) instrument. *Space*
898 *Sci. Rev.* **136**, 241-255.

899 Lin R. P. and Hudson H. S. (1976) Non-thermal processes in large solar flares. *Solar Physics* **50**, 153-178.

900 Malis T. F. and Steele, D. (1990) Ultramicrotomy for materials science. In: *Specimen Preparation for*
901 *Transmission Electron Microscopy II* (ed. R. Anderson), *MRS Symp. Proc.* **199**, Mat. Res. Soc.,
902 Pittsburgh, PA. pp. 3-42.

903 Matrajt G., Ito M., Wirick S., Messenger S., Brownlee D. E., Joswiak D., Flynn G. J., Sandford S. A., Snead
904 C. J. and Westphal A. J. (2008) Carbon investigation of two Stardust particles: a TEM, NanoSIMS,
905 and XANES study. *Meteorit. Planet. Sci.* **43**, 315-334.

906 McKeegan K. D., Aléon J., Bradley J. P., Brownlee D. E., Busemann H., Butterworth A., Chaussidon M.,
907 Fallon S., Floss C., Gilmour J., Gounelle M., Graham G. A., Guan Y., Heck P. R., Hoppe P.,
908 Hutcheon I. D., Huth J., Ishii H., Ito M., Jacobsen S. B., Kearsley A. T., Leshin L. A., Liu M., Lyon I.,

909 Marhas K., Marty B., Matrajt G., Meibom A., Messenger S., Mostefaoui S., Mukhopadhyay S.,
910 Nakamura-Messenger K., Nittler L. R., Palma R., Pepin R. O., Papanastassiou D. A., Robert F.,
911 Schlutter D., Snead C. J., Stadermann F. J., Stroud R., Tsou P., Westphal A. J., Young E. D., Ziegler
912 K., Zimmermann L. and Zinner E. (2006) Isotopic compositions of cometary matter returned by
913 Stardust. *Science* **314**, 1724-1728.

914 Messenger S. (2000) Identification of molecular-cloud material in interplanetary dust particles. *Nature*
915 **404**, 968-971.

916 Messenger S., Nakamura-Messenger K. and Keller L. P. (2008) ¹⁵N-rich organic globules in a cluster IDP
917 and the Bells CM2 chondrite. In: *Lunar Planet. Sci. XXXIX*. Lunar Planet. Inst., Houston, TX. #2391
918 (abstr.).

919 Millar T. J., Bennett A. and Herbst E. (1989) Deuterium fractionation in dense interstellar clouds.
920 *Astrophys. J.* **340**, 906-920.

921 Nakamura K., Zolensky M. E., Tomita S., Nakashima S. and Tomeoka K. (2003) Hollow organic globules in
922 the Tagish Lake meteorite as possible products of primitive organic reactions. *Int. J. Astrobiol.* **1**,
923 179-189.

924 Nakamura-Messenger K., Messenger S., Keller L. P., Clemett S. J. and Zolensky M. E. (2006) Organic
925 globules in the Tagish Lake meteorite: Remnants of the protosolar disk. *Science* **314**, 1439-1442.

926 Nichols R. H. Jr. (2006) Chronological constraints on planetesimal formation. In: *Meteorites and the*
927 *Early Solar System II* (eds. D. S. Lauretta and H. Y. McSween), Univ. Arizona Press, Tucson, AZ.
928 pp. 463-472.

929 Nittler L. R. (2003) Presolar stardust in meteorites: Recent advances and scientific frontiers. *Earth Planet.*
930 *Sci. Lett.* **209**, 259-273.

931 Noguchi T., Nakamura T., Okudaira K., Yano H., Sugita S. and Burchell M. J. (2007) Thermal alteration of
932 hydrated minerals during hypervelocity capture to silica aerogel at the flyby speed of Stardust.
933 *Meteorit. Planet. Sci.* **42**, 357-372.

934 Padovani M., Galli D. and Glassgold A. E. (2009) Cosmic-ray ionization of molecular clouds. *Astron.*
935 *Astrophys.* **501**, 619-631.

936 Robert F. and Epstein S. (1982) The concentration and isotopic composition of hydrogen, carbon and
937 nitrogen in carbonaceous meteorites. *Geochim. Cosmochim. Acta* **46**, 81-95.

938 Rodgers S. D. and Charnley S. B. (2008a) Nitrogen superfractionation in dense cloud cores. *Mon. Not.*
939 *Royal Astron. Soc. Lett.* **385**, L48-L52.

940 Rodgers S. D. and Charnley S. B. (2008b) Nitrogen isotopic fractionation of interstellar nitriles. *Astrophys.*
941 *J.* **689**, 1448-1455.

942 Rodgers S. D. and Charnley S. B. (2004) Interstellar diazenylium recombination and nitrogen isotopic
943 fractionation. *Mon. Not. Royal Astron. Soc.* **352**, 600-604.

944 Rosenberg R. A., Love P. J. and Rehn V. (1986) Polarization-dependent C(K) near-edge x-ray-absorption
945 fine structure of graphite. *Phys. Rev. B* **33**, 4034-4037.

946 Rotundi A., Baratta G. A., Borg J., Brucato J. R., Busemann H., Colangeli L., D'Hendecourt L., Djouadi Z.,
947 Ferrini G., Franchi I. A., Fries M., Grossemy F., Keller L. P., Mennella V., Nakamura K., Nittler L. R.,
948 Palumbo M. E., Sandford S. A., Steele A. and Wopenka B. (2008) Combined micro-Raman, micro-
949 infrared, and field emission scanning electron microscope analyses of comet 81P/Wild 2
950 particles collected by Stardust. *Meteorit. Planet. Sci.* **43**, 367-397.

951 Saito M. and Kimura Y. (2009) Origin of organic globules in meteorites: Laboratory simulation using
952 aromatic hydrocarbons. *Astrophys. J. Lett.* **703**, L147-L151.

953 Sandford S. A., Aléon J., Alexander C. M. O'D., Araki T., Bajt S., Baratta G. A., Borg J., Bradley J. P.,
954 Brownlee D. E., Brucato J. R., Burchell M. J., Busemann H., Butterworth A., Clemett S. J., Cody G.

955 D., Colangeli L., Cooper G., D'Hendecourt L., Djouadi Z., Dworkin J. P., Ferrini G., Fleckenstein H.,
956 Flynn G. J., Franchi I. A., Fries M., Gilles M. K., Glavin D. P., Gounelle M., Grossemy F., Jacobsen
957 C., Keller L. P., Kilcoyne A. L. D., Leitner J., Matrajt G., Meibom A., Mennella V., Mostefaoui S.,
958 Nittler L. R., Palumbo M. E., Papanastassiou D. A., Robert F., Rotundi A., Snead C. J., Spencer M.
959 K., Stadermann F. J., Steele A., Stephan T., Tsou P., Tyliczszak T., Westphal A. J., Wirick S.,
960 Wopenka B., Yabuta H., Zare R. N. and Zolensky M. E. (2006) Organics captured from comet
961 81P/Wild 2 by the Stardust spacecraft. *Science* **314**, 1720-1724.

962 Sandford S. A., Bernstein M. P., Allamandola L. J., Gillette J. S. and Zare R. N. (2000) Deuterium
963 enrichment of polycyclic aromatic hydrocarbons by photochemically induced exchange with
964 deuterium-rich cosmic ices. *Astrophys. J.* **538**, 691-697.

965 Sandford S. A., Bernstein M. P. and Dworkin J. P. (2001) Assessment of the interstellar processes leading
966 to deuterium enrichment in meteoritic organics. *Meteorit. Planet. Sci.* **36**, 1117-1133.

967 Schulz R., Jehin E., Manfroid J., Hutsemékers D., Arpigny C., Cochran A., Zucconi J. and Stüwe J. (2008)
968 Isotopic abundance in the CN coma of comets: Ten years of measurements. *Planet. Space Sci.*
969 **56**, 1713-1718.

970 Shard A. G., Whittle J. D., Beck A. J., Brookes P. N., Bullett N. A., Talib R. A., Mistry A., Barton D. and
971 McArthur S. L. (2004) A NEXAFS examination of unsaturation in plasma polymers of allylamine
972 and propylamine. *J. Phys. Chem. B* **108**, 12472-12480.

973 Simnett G. M., Roelof E. C. and Haggerty D. K. (2002) The acceleration and release of near-relativistic
974 electrons by coronal mass ejections. *Astrophys. J.* **579**, 854-862.

975 Skytt P., Glans P., Mancini D. C., Guo J., Wassdahl N., Nordgren J. and Ma Y. (1994) Angle-resolved soft-x-
976 ray fluorescence and absorption study of graphite. *Phys. Rev. B* **50**, 10457-10461.

977 Stadermann F. J., Hoppe P., Floss C., Heck P. R., Hörz F., Huth J., Kearsley A. T., Leitner J., Marhas K. K.,
978 McKeegan K. D. and Stephan T. (2008) Stardust in Stardust--The C, N, and O isotopic
979 compositions of Wild 2 cometary matter in Al foil impacts. *Meteorit. Planet. Sci.* **43**, 299-313.
980 Strazzulla G. and Baratta G. A. (1992) Carbonaceous material by ion irradiation in space. *Astron.*
981 *Astrophys.* **266**, 434-438.
982 Strong A. W., Moskalenko I. V. and Reimer O. (2000) Diffuse continuum gamma rays from the galaxy.
983 *Astrophys. J.* **537**, 763-784.
984 Stroud R. M., Long J. W., Pietron J. J. and Rolison D. R. (2004) A practical guide to transmission electron
985 microscopy of aerogels. *J. Non-Cryst. Solids* **350**, 277-284.
986 Terzieva R. and Herbst E. (2000) The possibility of nitrogen isotopic fractionation in interstellar clouds.
987 *Mon. Not. Royal Astron. Soc.* **317**, 563-568.
988 Tielens A. G. G. M. (1983) Surface chemistry of deuterated molecules. *Astron. Astrophys.* **119**, 177-184.
989 Urquhart S. G. and Ade H. (2002) Trends in the carbonyl core (C 1S, O 1S) $\rightarrow \pi^*_{C=O}$ transition in the near-
990 edge X-ray absorption fine structure spectra of organic molecules. *J. Phys. Chem. B* **106**, 8531-
991 8538.
992 Weng X., Rez P. and Ma H. (1989) Carbon K-shell near-edge structure: Multiple scattering and band-
993 theory calculations. *Phys. Rev. B* **40**, 4175-4178.
994 Wessely O., Katsnelson M. I. and Eriksson O. (2005) Ab initio theory of dynamical core-hole screening in
995 graphite from X-ray absorption spectra. *Phys. Rev. Lett.* **94**, 167401.
996 Wood B. E., Müller H.-R., Zank G. P. and Linsky J. L. (2002) Measured mass-loss rates of solar-like stars.
997 *Astrophys. J.* **574**, 412-425.
998 Yoshida K. (2008) High-energy cosmic-ray electrons in the galaxy. *Adv. Space Res.* **42**, 477-485.
999 Zolensky M. E., Zega T. J., Yano H., Wirick S., Westphal A. J., Weisberg M. K., Weber I., Warren J. L.,
1000 Velbel M. A., Tsuchiyama A., Tsou P., Toppani A., Tomioka N., Tomeoka K., Teslich N., Taheri M.,

1001 Susini J., Stroud R., Stephan T., Stadermann F. J., Snead C. J., Simon S. B., Simionovici A., See T.
1002 H., Robert F., Rietmeijer F. J. M., Rao W., Perronnet M. C., Papanastassiou D. A., Okudaira K.,
1003 Ohsumi K., Ohnishi I., Nakamura-Messenger K., Nakamura T., Mostefaoui S., Mikouchi T.,
1004 Meibom A., Matrajt G., Marcus M. A., Leroux H., Lemelle L., Le L., Lanzirotti A., Langenhorst F.,
1005 Krot A. N., Keller L. P., Kearsley A. T., Joswiak D., Jacob D., Ishii H., Harvey R., Hagiya K.,
1006 Grossman L., Grossman J. N., Graham G. A., Gounelle M., Gillet P., Genge M. J., Flynn G. J.,
1007 Ferroir T., Fallon S., Ebel D. S., Dai Z. R., Cordier P., Clark B. C., Chi M., Butterworth A. L.,
1008 Brownlee D. E., Bridges J. C., Brennan S., Brearley A., Bradley J. P., Bleuet P., Bland P. A. and
1009 Bastien R. (2006) Mineralogy and petrology of comet 81P/Wild 2 nucleus samples. *Science* **314**,
1010 1735-1739.

1011 Zubavichus Y., Fuchs O., Weinhardt L., Heske C., Umbach E., Denlinger J. D. and Grunze M. (2004) Soft X-
1012 ray-induced decomposition of amino acids: An XPS, mass spectrometry, and NEXAFS study.
1013 *Radiat. Res.* **161**, 346-358.

1014
1015

1016 FIGURE CAPTIONS

1017 **Figure 1.** TEM (left-most column) and STXM (middle left column) images and SIMS maps of CN⁻ (middle
1018 right column) and $\delta^{15}\text{N}$ or δD (right-most column) of extraterrestrial carbonaceous samples in this study
1019 **(A)** Track 80 organic section in Stardust sample C2092,6,80,43,2. Cometary organic matter is
1020 concentrated in the center of the section (bounded by dashed lines), while both aerogel and cometary
1021 organic matter are present at the two ends of the section. This division is also visible in the SIMS images.
1022 **(B)** Track 80 globule section in the same sample. **(C)** Track 2 globule in Stardust sample FC3,0,2,4,5. The
1023 SIMS δD image has been digitally smoothed to improve the statistical significance of the color scale. **(D)**
1024 Two organic globules (M1 and M2) found in the IOM residue from the Murchison meteorite.

1025

1026 **Figure 2.** Carbon XANES of cometary and meteoritic globules compared to bulk IOM from Murchison. **(A)**
1027 Spectrum from the Track 80 organic section in Figure 1A. **(B)** Spectrum from the Track 80 globule in
1028 Figure 1B. **(C)** Spectrum from the larger Murchison globule (M1) in Figure 1D. **(D)** Spectrum from the
1029 smaller Murchison globule (M2) in Figure 1D.

1030

1031 **Figure 3.** Carbon and nitrogen K-edge XANES spectra of the Track 2 globule. C-XANES spectrum of the
1032 organic globule **(A)** before and **(B)** after TEM imaging, compared with a standard sample of
1033 cyanoacrylate adhesive. **(C)** N-XANES spectrum of the globule after TEM imaging.

1034

1035 **Figure 4.** NanoSIMS images of TEM-irradiated cyanoacrylate adhesive and epoxy. **(A)** Secondary electron
1036 image of ultramicrotomed cyanoacrylate showing a rectangular region of STEM damage. **(B)** δD map
1037 (corresponding to the white square in **A**) showing enhanced D in the damaged region. **(C)** Secondary
1038 electron image of ultramicrotomed epoxy showing nearby regions of STEM and TEM damage. **(D)** δD
1039 map (corresponding to the white square in **C**) showing enhanced D in a 1.5 μm spot from TEM damage.

1040

1041 **Figure 5.** Average ^{15}N and D isotopic compositions of cometary globules from this study compared with
1042 organic matter in other planetary materials. The $\delta^{15}\text{N}$ value of the Track 80 globule plots near those of a
1043 Stardust Al foil crater and an isotopically anomalous region of organic matter in an interplanetary dust
1044 particle. References: ^aSchulz et al. (2008), ^bMcKeegan et al. (2006), ^cMatrajt et al. (2008), ^dNakamura-
1045 Messenger et al. (2006), ^eFloss and Stadermann (2009), ^fBusemann et al. (2006), ^gFloss et al. (2004),
1046 ^hAlexander et al. (2007).

1047

1048

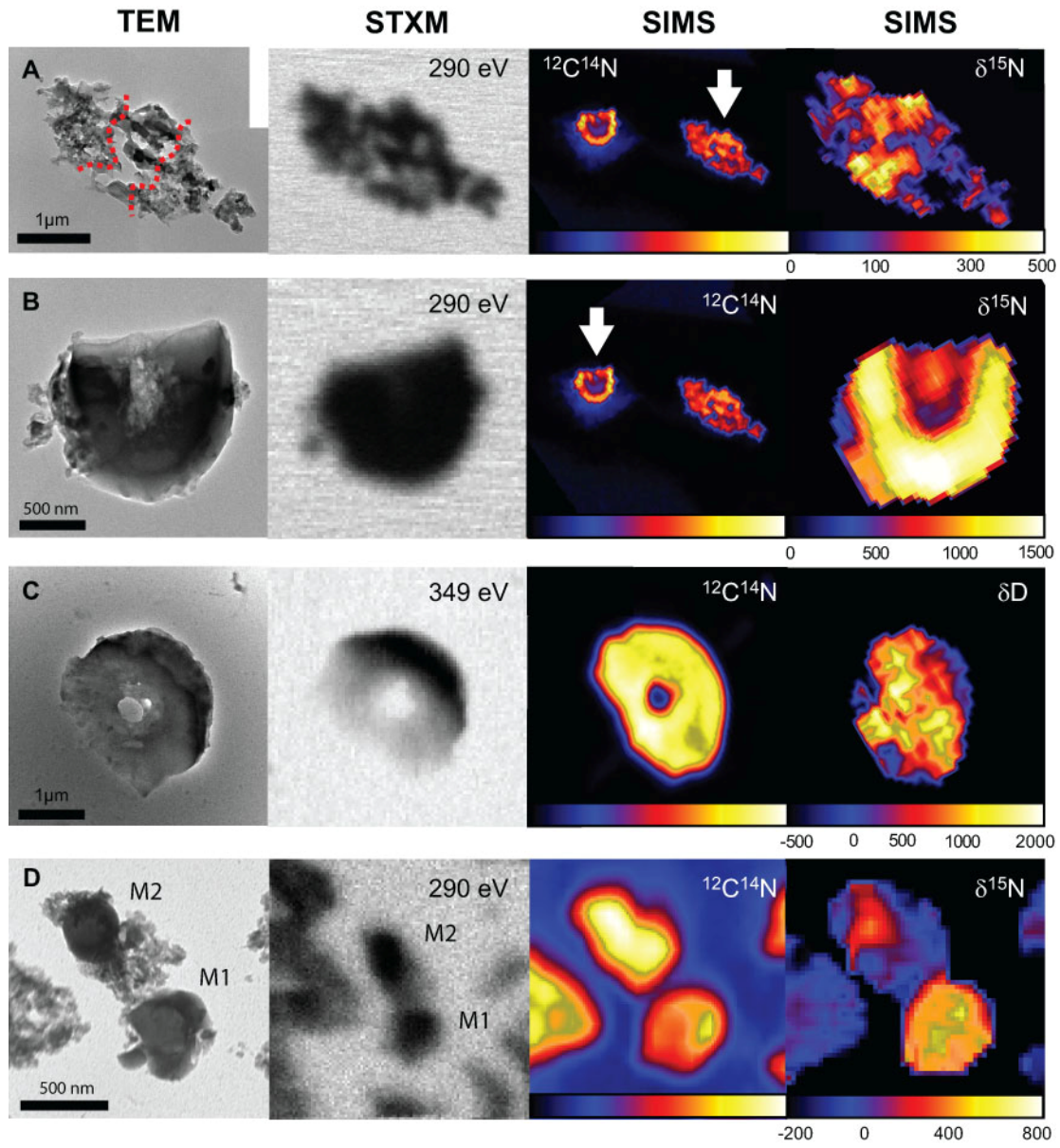
1049 TABLES

1050 Table 1. Isotopic composition and atomic N/C ratios of samples in this study

Sample	δD (‰)	$\delta^{13}C$ (‰)	$\delta^{15}N$ (‰)	N/C
C2092,6,80,43,2 (aerogel-rich)	n.m.	-42 ± 14	$+136 \pm 15$	0.1 - 0.15
C2092,6,80,43,2 (globule)	< +1000	-77 ± 13	$+1120 \pm 30$	0.1 - 0.15
FC3,0,2,4,5	$+1000 \pm 170$	-35 ± 3	-7 ± 5	0.08 - 0.16
Murchison (large globule)	n.m.	n.m.	$+470 \pm 35$	n.m.
Murchison (small globule)	n.m.	n.m.	$+289 \pm 39$	n.m.
Murchison (bulk IOM) ^a	+777	-19	-1	0.03
Cyanoacrylate (STEM)	+500 - +800	n.m.	-2 ± 5	n.m.
Epoxy (TEM)	+1000	n.m.	n.m.	n.m.
Epoxy (STEM)	> +150	n.m.	n.m.	n.m.

1051 n.m. = not measured

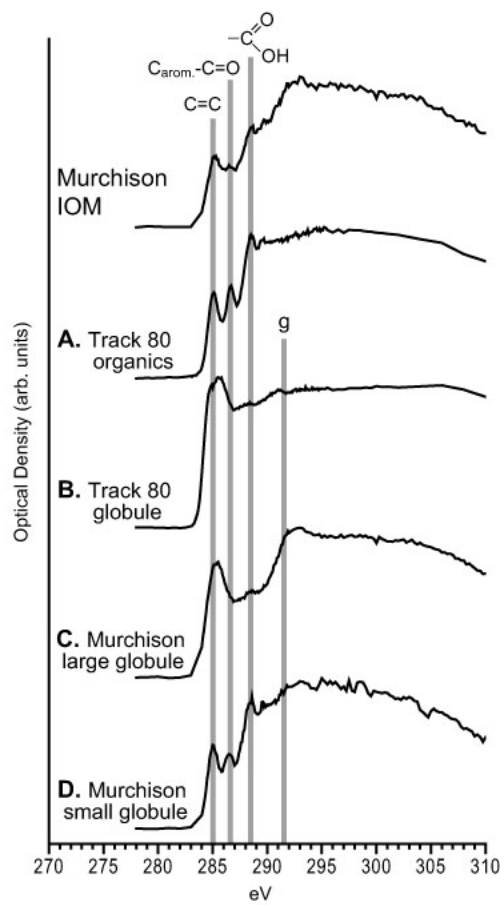
1052 (a) Data from Alexander et al. (2007).



1054

1055 FIGURE 1

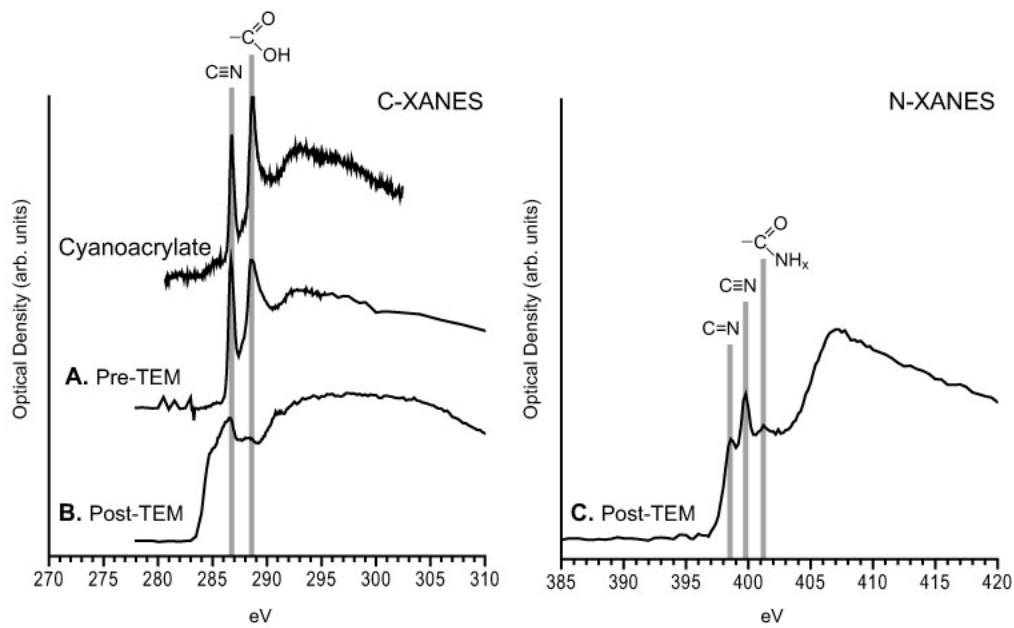
1056



1057

1058 FIGURE 2

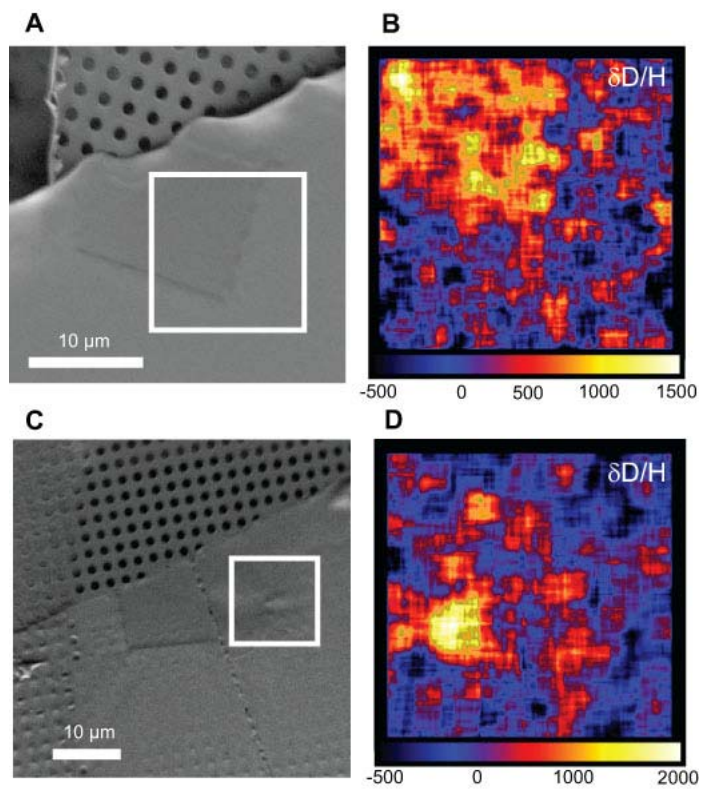
1059



1060

1061 FIGURE 3

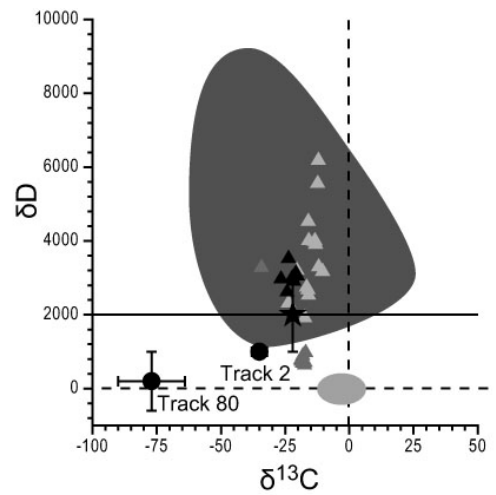
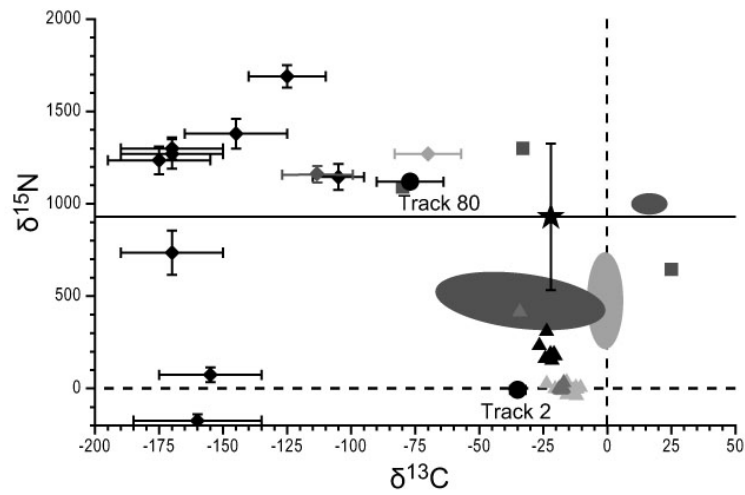
1062



1063

1064 FIGURE 4

1065



- ★ Comets^a
- Wild 2 globules
- Wild 2 "hotspots"^b
- Wild 2 organic matter^c
- Tagish Lake globules^d
- ◆ QUE 99177 "hotspots"^e
- ◆ EET 92042 "hotspot"^f
- ◆ IDP "hotspot"^g
- ▲ CR chondrites^h
- ▲ CM/CI chondrites^h
- ▲ Ordinary chondrites^h

1066

1067 FIGURE 5